Structural Engineering and Mechanics, *Vol. 69, No. 2 (2019) 205-219*
DOI: https://doi.org/10.12989/sem.2019.69.2.205

Nonlinear vibration of functionally graded nano-tubes using nonlocal strain gradient theory and a two-steps perturbation method

Yang Gao[1,2], Wan-Shen Xiao*[1,2] and Haiping Zhu[3]

[1]*State Key Laboratory of Advanced Design and Manufacturing for Vehicle Body, Hunan University, Changsha 410082, China*
[2]*College of Mechanical and Vehicle Engineering, Hunan University, Changsha 410082, China*
[3]*School of Computing, Engineering and Mathematics, Western Sydney University, Locked, Bag 1797, Penrith, NSW 2751, Australia*

(Received August 24, 2018, Revised November 13, 2018, Accepted December 14, 2018)

Abstract. This paper analyzes nonlinear free vibration of the circular nano-tubes made of functionally graded materials in the framework of nonlocal strain gradient theory in conjunction with a refined higher order shear deformation beam model. The effective material properties of the tube related to the change of temperature are assumed to vary along the radius of tube based on the power law. The refined beam model is introduced which not only contains transverse shear deformation but also satisfies the stress boundary conditions where shear stress cancels each other out on the inner and outer surfaces. Moreover, it can degenerate the Euler beam model, the Timoshenko beam model and the Reddy beam model. By incorporating this model with Hamilton's principle, the nonlinear vibration equations are established. The equations, including a material length scale parameter as well as a nonlocal parameter, can describe the size-dependent in linear and nonlinear vibration of FGM nanotubes. Analytical solution is obtained by using a two-steps perturbation method. Several comparisons are performed to validate the present analysis. Eventually, the effects of various physical parameters on nonlinear and linear natural frequencies of FGM nanotubes are analyzed, such as inner radius, temperature, nonlocal parameter, strain gradient parameter, scale parameter ratio, slenderness ratio, volume indexes, different beam models.

Keywords: functionally graded material; nonlinear vibration; nonlocal strain gradient theory; nanotubes

1. Introduction

The rapid development of industry puts forward higher requirements for material performance so that various composites have been manufactured and developed in the past several decades, such as functionally graded materials (FGMs), fiber reinforced composites, carbon nanotubes reinforced composites (CNTRCs). Among these composite materials, functionally graded material (FGM) in which the effective material properties can be changed in a certain direction have captured extensive attention in a multitude of industries (Koizumi 1997, Hichem *et al.* 2017, Abdelaziz *et al.* 2017, Bellifa *et al.* 2016, Meziane *et al.* 2014, Ahouel *et al.* 2016). Mahi *et al.* (2015) used a new hyperbolic shear deformation theory which includes five degrees of freedom to study functionally graded sandwich as well as laminated composite pales. Yahia *et al.* (2015) developed various higher-order shear deformation plate theories for wave propagation, then used them to undertake wave dispersion of functionally graded materials. Besides, another developed shear deformation theory where the number of unknowns and governing equations are reduced, was utilized to study wave propagation of functionally graded plate in thermal environment (Boukhari *et al.* 2016). Based on a novel four variable refined plate theory, Merdaci *et al.* (2016) proposed the analytical solutions of functionally graded plates under antisymmetric cross-ply and angle-ply in analysis of bending and buckling of FG plates.

When analyzing problems of functionally graded materials, those classic theories, like Euler-Bernoulli beam model, Timoshenko beam model and Reddy beam model, ought to be modified, because constituents of FGMs vary continuously in the the certain direction whereas material is supposed to be homogeneous within the theoretical framework of classic theories (Bousahla *et al.* 2014, Zaoui *et al.* 2019, Hamidi *et al.* 2015, Bennoun *et al.* 2016, Bourada *et al.* 2015, Belabed *et al.* 2014, Younsi *et al.* 2018, Bouafia *et al.* 2017). Kaci *et al.* (2018) used a novel theory of higher order shear deformation to undertake the analysis of post-buckling of composite beams, which is better than the case of other classic beam model. Zidi *et al.* (2017) proposed a novel simple higher-order shear deformation theory without needing a shear correction factor for FG beams where the results of bending and vibration analysis were more accurate than Timoshenko beam model. Moreover, Mouffoki *et al.* (2017) put forward a new two-unknown trigonometric shear deformation beam theory to study vibration of nonlocal advanced nanobeams in hygro-thermal environment. Differing from the above theories, Houari *et al.* (2016) and Belabed *et al.* (2018) respectively developed a new simple three-unknown sinusoidal shear deformation theory and a new 3-unknown hyperbolic shear deformation theory for functionally graded plates, then the results obtained by both novel theories are not only simple

*Corresponding author, Professor
E-mail: xwshndc@126.com

ISSN: 1225-4568 (Print), 1598-6217 (Online)

in analyzing the bending behaviors of FG plates, but also superior than the conventional higher-order shear deformation theories that includes more number of unknowns.

Owing to functionally graded materials related to temperature variation, thermal effect on structural components made of functionally graded materials should be discussed in detail. Bouderba *et al.* (2016) and Bouderba *et al.* (2013) separately studied thermal buckling response of FG plates and thermal bending of FG plates using a simple first order shear deformation theory. El-Haina *et al.* (2017) attempted to present a simple analytical approach to analyze the thermal buckling behaviors of FG plates. Besides, for functionally graded plates subjected to uniform, linear and nonlinear thermal loads, Menasria *et al.* (2017) used a new displacement field that contains undetermined integral terms to study thermal buckling and Bousahla *et al.* (2016) used a four-variable refined plate theory to account for transverse shear strains. Meanwhile, a series of researches relevant to linear and nonlinear bending of functionally graded plates were carried out, including Hamidi *et al.* (2015), Tounsi *et al.* (2013), Zidi *et al.* (2014), Beldjelili *et al.* (2016), Attia *et al.* (2018).

Such materials are fabricated into different structural components, e.g., plates, rods and tubes. Thereinto, tube is one of the most important and frequently used structural components in many industries. Fig. 1 shows some potential fields for functionally graded materials as well as tubes application (Dai *et al*. 2016, Jha *et al*. 2013, Dohmann and Hartl 1997, Dresselhaus *et al*. 2004, Ebrahimi and Javari 2016, Zouatnia *et al.* 2017, Gan 2016). Up to now, a multitude of researchers have reported analyses on mechanical behaviors of tubes made of functionally graded materials in open literatures. Hu *et al*. (2017) put forward a complex structure preserving method to study axial dynamic buckling of carbon nano-tubes with a small angle in the direction of axle, which can give guidance for the experimental approach. A higher order shear deformation beam model for tubes was tailored by Zhang and Fu (2013), which can make the shear stress boundary conditions cancel out on the surface of tubes. Afterwards, Gui-Lin She and Wan-Shen Xiao undertook linear vibration of tubes (She *et al*. 2018) as well as thermal buckling of porous tubes (She *et al*. 2017) with the aid of a refined beam model from Zhang and Fu (2013). In these researches, obtaining analytical solutions from their mathematical models is a key step.

Scholars have developed various methods to solve equations of linear and non-linear in order to obtain corresponding analytical solutions, such as high dimensional harmonic balance method (Hall *et al*. 2002, Liu *et al*. 2007), harmonic balance method (Liu and Dowell 2004, Dai *et al*. 2014) and perturbation methods (Mook and ANayfeh 1979). Perturbation methods are frequently used. Nazemnezhad and Hosseini (2014) studied non-linear free vibration of FG beams under different boundary conditions with the aid of the multiple-scale perturbation method. Ghadiri *et al*. (2017) used Euler-Bernoulli beam model to analyze forced vibration of beams subjected to moving concentrated load, where to obtain analytical solution from

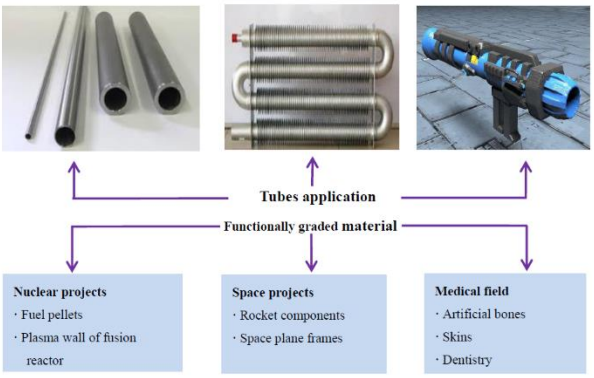

Fig. 1 Potential fields for functionally graded material and tubes application

non-linear differential equations, the perturbation technique was employed to achieve this. Shen and Wang (2014) used perturbation method, namely a two-steps perturbation technique, to investigate vibration of beams exposed to different types of thermal environment. Through comparing and studying results of various perturbation methods, we adopt a two-steps perturbation technique to undertake the analysis of nanotubes in this paper.

In analysis of problems involving nano-structures, the effect of size-dependent becomes overwhelmingly important on the mechanical behaviors, which has been observed and corroborated by experimental findings. However, those classical theories cannot capture the size effect at nanoscale for sake of other length-scale parameters. Later on, to resolve this difficulty, some researchers put forward various size-dependent continuum models to study the mechanical behaviors of nanostructures, including nonlocal elasticity theory, the strain gradient theory and nonlocal strain gradient theory.

The nonlocal elasticity theory supposes that the stress at any point in a body varies along with not only the strain at that point but also those at all other points of the body. Since this theory being proposed by Eringen (1972), a multitude of researches have been performed in order to describe the size effect on nanostructurs and give its reasons. Rahmani and Pedram (2014) analyzed the size-dependent effect on the vibration of FGM nano-beams by utilizing non-local elasticity theory and obtained a closed form solution. A nonlocal zeroth-order shear deformation theory was used to study free vibration of FG plates (Bounouara *et al.* 2016) and nonlinear post-buckling of beams (Bellifa *et al.* 2017).

Salehipour *et al*. (2015) modified the non-local elasticity theory in analysis of FGM at nanoscale. The influence of non-local parameter was analyzed in detail based on an improved non-local elasticity theory. Ansari *et al*. (2015) dealt with nonlinear forced vibration of magneto-electro-thermo-elastic beams based on a third-order deformable model and the nonlocal elasticity theory. With the development of the nonlocal elasticity theory, plenty of scholars proposed a variety of modified nonlocal elasticity theory, then used them to capture the size-dependent on the nanometer length (Yazid *et al.* (2018), Bouafia *et al.* 2017, Ahmed *et al.* 2018, Besseghier *et al.* 2017, Khetir *et al.*

2017, Belkorissat *et al.* 2015, Zemri *et al.* 2015). Besides, in terms of the Eringen's theory, many studies have demonstrated that surface energy play an important effect on nanostructures, such as Youcef *et al.* (2018), Hamzacherif *et al.* (2018), Mouffoki *et al*. (2017), Chaht *et al.* (2015). Differing from above references adopted Eringen's equivalent differential formulation, Tuna and Kirca (2016) analyzed buckling and vibration of beams by using the original integral constitutive equation. In order to obtain the exact solution of the original integral model, the Laplace transform method was adopted to solve several governing equations. Additionally, Faghidian (2018), Khodabakhshi and Reddy (2015) and Fernández-Sáez (2016) utilized the original integral model to analyze the size effect.

Although the nonlocal elasticity theory has successfully described the size-dependent, it merely characterizes the effect of stiffness-softening. As for the effect of stiffness-hardening on nanostructures reported by theoretical as well as experimental researches (Fleck and Hutchinson 2001, Yang *et al*. 2002), the nonlocal elasticity theory doesn't hold up. To resolve this problem, the strain gradient theory (Mindlin 1964, Mindlin 1965) proposed by Mindin is another microsructure dependent continuum theory, which can take the stiffness enhancement into account. The theory assumes that additional strain gradient terms ought to be incorporated in the total stress field when analyzing mechanism of nano-sturctural deformation. Based on Mindin's theory, Lam *et al*. (2003) proposed a modified strain gradient theory in which double classical material length-scale parameters and three non-classical ones are taken into consideration. It should be mentioned out that determining non-classical parameters is a difficult work in the above-mentioned theories. Consequently, additional modified couple stress theory was tailored by Yang *et al*. (2009) in which the number of non-classical material length scale parameter is reduced to one. As a matter of fact, this modified couple stress theory is a special case of the modified strain gradient theory from the perspective of strain energy density. Later on, on the basis of these modified theories, a lot of studies have been carried out. Thereinto, the effect of stiffness-hardening can be observed in the vibration of plates (Tsiatas 2009, Reddy *et al*. 2015, Şimşek *et al*. 2015, Li and Pan 2015), beams with cross section (Bekir and Ömer 2011, Ma *et al*. 2008, Al-Basyouni *et al.* 2015) as well as circular cylindrical beams (Bekir *et al*. 2013, Bekir and Ömer 2014, Rahaeifard 2015).

From what has been surveyed above, we can know that the strain gradient theory aligned with the nonlocal elasticity theory are two different non-classical theories to describe the effect of size-dependent on nanostructures, then give its reasons. In order to simultaneously evaluate the two size-dependent effect on small scaled structures, Lim *et al*. (2015) put forward nonlocal strain gradient model which combines the strain gradient theory and the nonlocal elasticity theory, together. So far, some studies with respect to the mechanical behaviors of nano-structures have been performed based on the nonlocal strain gradient theory. Lu *et al*. (2017) developed a size-dependent sinusoidal shear deformation model to study free vibration of beams with the aid of the theory. Li *et al*. (2016) used it to undertake the analysis of longitudinal vibration of nanorods. Karami *et al.* (2018a) and Karami *et al.* (2018b) in analysis of the wave dispersion in anisotropic doubly-curved nanoshells presented the influence of strain gradient stress field and nonlocal elastic stress field. Ebrahimi and Barati (2017) and Li *et al*. (2017) studied vibration of axially graded beams in the framework of nonlocal strain gradient elasticity theory. Karami *et al*. (2017) for the first time combined nonlocal strain gradient theory with three dimensional elasticity theory together to investigate the wave propagation behaviors of plates. Then, She *et al*. (2018) investigated wave propagation in porous nanotubes with the guidance of the theory. Sahmani *et al*. (2018) employed this theory to explore the size-dependent in large amplitude of functionally graded porous plates. However, there are only few studies relevant to nonlinear nanostructures, especially nonlinear nanotubes.

Consequently, this paper analyzes nonlinear free vibration of the circular nano-tubes made of functionally graded materials in the framework of nonlocal strain gradient theory in conjunction with a refined beam model proposed by Zhang and Fu (2013). Firstly, a higher-order shear deformation theory which can degenerate into the Euler beam model, the Timoshenko beam model and the Reddy beam model is used to formulate the mechanical model, and the nonlinear strain-displacement relationships is also considered. Secondly, via using a two-steps perturbation method, the analytical solution is obtained from nonlinear governing equations. Thirdly, the effects of various physical parameters on nonlinear and linear natural frequencies of FGM nanotubes are analyzed, the findings of which are different from previous results.

2. Basic theoretical formulation

2.1 Functionally graded tubes

Note that a functionally graded tube with outer radius R_0, inner radius R_i, as well as length L shown in Fig. 2 is subjected to a uniform pressure and exposed to thermal environment. Consider that its middle-axis coincides with the *Ox*-axis of a Cartesian coordinate system *O-xyz* and the positive *Z*-axis is perpendicular to the *X*-axis and directed upwards. The origin of a Cartesian coordinate system *O-xyz* is set at the middle surface of the tube. It can be seen that $y = r\cos(\varphi), z = r\sin(\varphi)$ as well as $r^2 = y^2 + z^2$. Thus, the effective material properties P_f of the FGM tube, stating Young's modulus, thermal expansion, Poisson's ratio, as well as mass density, on the basis of the power-law, can be expressed as (Zhong *et al*. 2016)

$$P_f = p_1 + (p_2 - p_1)\left(\frac{r - R_i}{R_0 - R_i}\right)^N \tag{1}$$

where p_1, p_2 stand for respective material constituents of SUS304 and Si_3N_4. The symbol of N represents the volume fraction index. The temperature factor is assumed to be a nonlinear function of temperature, which can be described

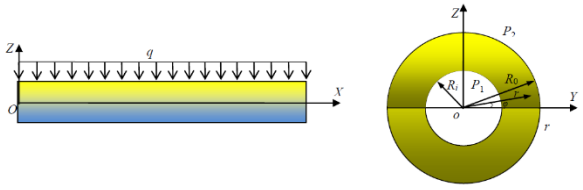

Fig. 2 Geometry and coordinate of functionally graded tubes

as (Ghiasian *et al*. 2014)

$$P(T)=P_0\left(P_{-1}T^{-1}+1+P_1T+P_2T^2+P_3T^3\right) \tag{2}$$

in which P_0, P_{-1}, P_1, P_2, and P_3 denote the coefficients of Kelvin's temperature-dependence which are tabulated in Table 1. Notice from the effective material properties P_f that inner surface (r=R_i) of FGM tube is made of SUS304, whereas outer surface (r=R_0) of FGM tube is made of Si_3N_4.

2.2 Nonlocal strain gradient theory

When dealing with nano-structures, the effect of size-dependent can't be ignored in the process of analysis. Lim *et al*. (2015) put forward the nonlocal strain gradient theory involving the nonlocal elastic theory aligned with the strain gradient theory. According to this theory, the total stress tensor can be defined as

$$t_{xx}=\sigma_{xx}-\frac{\mathrm{d}\sigma_{xx}^{(1)}}{\mathrm{d}x} \tag{3}$$

in which the classical stress σ_{xx} and the higher order stress tensor $\sigma^{(1)}$ associated with strain ε_{xx} and strain gradient $\varepsilon_{xx,x}$ can be given by

$$\sigma_{xx}=\int_0^L E(x)\alpha_0\left(x,x',e_0a\right)\varepsilon'_{xx}\left(x'\right)\mathrm{d}x' \tag{4}$$

$$\sigma_{xx}^{(1)}=l^2\int_0^L E(x)\alpha_1\left(x,x',e_1a\right)\varepsilon'_{xx}\left(x'\right)\mathrm{d}x' \tag{5}$$

where $\alpha_0\left(x,x',e_0a\right)$ and $\alpha_1\left(x,x',e_1a\right)$ are the two non-local kernel functions that satisfy certain conditions of Eringen (1983). Thereinto, both nonlocal parameters e_0a and e_1a are used to take into account the importance of nonlocal elastic stress field. Owing to attenuation functions for classical stresses aligned with higher order stresses being the same, we suppose e_0a=e_1a=ea in this paper. Moreover, $E(x)$ and L denote Yong's modulus and the length of tube, respectively.

However, it is difficult to obtain analytical results by applying the above expressions. Therefore, Lim *et al*. (2015) suggested a simplification, turning the integral constitutive relations to an equivalent differential form as

$$\left(1-(ea)^2\nabla^2\right)\sigma_{xx}=E(x)\varepsilon_{xx} \tag{6}$$

$$\left(1-(ea)^2\nabla^2\right)\sigma_{xx}^{(1)}=l^2E(x)\varepsilon_{xx,x} \tag{7}$$

in which $\nabla=\partial/\partial x$.

Submitting Eq. (6) into Eq. (7), we could obtain the general nonlocal strain gradient constitutive equation.

$$\left[1-(ea)^2\nabla^2\right]t_{xx}=E(x)\varepsilon_{xx}-l^2\nabla\cdot\left(E(x)\nabla\varepsilon_{xx}\right) \tag{8}$$

It should be mentioned out that the Eq. (8) can degenerate the following two models.

The Eringen's nonlocal elasticity theory: By setting l=0, the Eq. (8) can naturally degenerate the nonlocal elasticity constitutive equation (Eringen 1983, Eringen 1972).

$$\left[1-(ea)^2\nabla^2\right]t_{xx}=E(x)\varepsilon_{xx} \tag{9}$$

The strain gradient theory: By setting ea=0, the Eq. (8) can naturally degenerate the pure strain gradient constitutive equation (Aifantis 1992).

$$t_{xx}=E(x)\varepsilon_{xx}-l^2\nabla\cdot\left(E(x)\nabla\varepsilon_{xx}\right) \tag{10}$$

It can be seen that the Eq. (8) can explain the effect of size-dependent, reasonably.

3. Mathematical model

Considering the circular tube, three displacement functions (u_1, u_2, u_3) can be listed as follows (Zhang and Fu 2013)

$$\begin{aligned}u_1&=u(x,t)+f\left(y,z\right)\frac{\partial w(x,t)}{\partial x}+g(y,z)\theta(x,t)\\u_2&=0\\u_3&=w(x,t)\end{aligned} \tag{11}$$

in which

$$f\left(y,z\right)=\frac{z}{R_0^2+R_i^2}\left(\frac{R_0^2R_i^2}{r^2}-\frac{r^2}{3}\right)$$
$$g\left(y,z\right)=f+z$$

where $u(x,t)$ and $w(x,t)$ respectively stand for double displacement components of any point in the axial (X) and lateral (Z) and $\theta(x,t)$ states the rotation of the normal relative to the Y axis.

Next, the nonlinear strain-displacement expressions in line with the von karman non-linearity theory can be induced as

$$\begin{aligned}\varepsilon_x&=\frac{\partial u}{\partial x}+\frac{1}{2}\left(\frac{\partial w}{\partial x}\right)^2+f\frac{\partial^2 w}{\partial x^2}+g\frac{\partial\theta}{\partial x};\\\gamma_{xy}&=\frac{\partial f}{\partial y}\frac{\partial w}{\partial x}+\frac{\partial g}{\partial y}\theta\\\gamma_{xz}&=\frac{\partial f}{\partial z}\frac{\partial w}{\partial x}+\frac{\partial g}{\partial z}\theta+\frac{\partial w}{\partial x}=\frac{\partial g}{\partial z}\left(\frac{\partial w}{\partial x}+\theta\right)\\\gamma_{xr}&=\gamma_{xz}\sin\left(\varphi\right)+\gamma_{xy}\cos\left(\varphi\right)\end{aligned} \tag{12}$$

where ε_{xx}, γ_{xy}, γ_{xz}, and γ_{xr} are normal strain, respective engineering shear strain in the direction of axis(Y) and axis(Z) as well as radial strain. According to the Hooke's law, the stresses associated with strain components from Eq.

(12) can be determined as Eq. (13) in a uniform thermal environment.

$$\left(\sigma_x,\tau_{xy},\tau_{xz},\tau_{xr}\right)=\left(E_f\varepsilon_x-E_f\alpha_x\Delta T,G_f\gamma_{xy},G_f\gamma_{xz},G_f\gamma_{xr}\right) \tag{13}$$

in which

$$G_f=\frac{E_f}{2\left(1+\nu_f\right)}$$

The necessary boundary conditions for the stress of the tube at the (r=R_0, R_i) must satisfy Eq. (14).

$$\tau_{xr}\mid_{r=R_i,R_0}=0 \tag{14}$$

The variation of virtual strain energy of the tube is assumed to be

$$\delta\Pi_s=\int_\Omega\left(\sigma_x\delta\varepsilon_x+\tau_{xz}\delta\gamma_{xz}+\tau_{xy}\delta\gamma_{xy}\right)\mathrm{d}\Omega \tag{15}$$

in which Ω stands for the volume of the tube. By submitting Eq. (12) into Eq. (15), the variation of the virtual strain energy is reappraised as

$$\delta\Pi_s=\int_\Omega\left\{\sigma_x\delta\left[\frac{\partial u}{\partial x}+\frac{1}{2}\left(\frac{\partial w}{\partial x}\right)^2+f\frac{\partial^2 w}{\partial x^2}+g\frac{\partial\theta}{\partial x}\right]+\tau_{xz}\delta\left[\frac{\partial g}{\partial z}\left(\frac{\partial w}{\partial x}+\theta\right)\right]+\tau_{xy}\delta\left(\frac{\partial f}{\partial y}\frac{\partial w}{\partial x}+\frac{\partial g}{\partial y}\theta\right)\right\}\mathrm{d}\Omega \tag{16}$$

Besides, the variation of the virtual work performed by the external force is illustrated as

$$\delta\Pi_W=-\int_0^L\left[q\delta w+N_T\frac{\partial w}{\partial x}\delta\left(\frac{\partial w}{\partial x}\right)\right]\mathrm{d}x \tag{17}$$

The variation of kinetic energy of the tube is written as

$$\delta\Pi_T=\int_\Omega\rho_f\delta\left[\frac{1}{2}\left(\frac{\partial u_1}{\partial t}\right)^2+\frac{1}{2}\left(\frac{\partial u_3}{\partial t}\right)^2\right]\mathrm{d}\Omega \tag{18}$$

So, Eq. (18) can be deduced as

$$\delta\Pi_T=\int_\Omega\frac{1}{2}\rho_f\left\{\delta\left[f^2\left(\frac{\partial^2 w}{\partial x\partial t}\right)^2\right]+\delta\left[g^2\left(\frac{\partial\theta}{\partial t}\right)^2\right]+\delta\left[2fg\frac{\partial^2 w}{\partial x\partial t}\frac{\partial\theta}{\partial t}\right]+\delta\left(\frac{\partial w}{\partial t}\right)^2\right\}\mathrm{d}\Omega \tag{19}$$

In terms of the Hamilton principle, the corresponding governing equations can be induced as

$$\delta\Pi=\delta\left(\Pi_s+\Pi_w-\Pi_T\right)=0 \tag{20}$$

When to take Eq. (16), Eq. (17) and Eq. (19) into Eq. (20) and set these coefficients of δu, $\delta\theta$, δw into zero, the nonlinear equilibrium equations can be expressed as

$$\begin{aligned}&\frac{\mathrm{d}N}{\mathrm{d}x}=0\\&\frac{\partial M}{\partial x}-Q-I_2\frac{\partial^3 w}{\partial x\partial t^2}-I_3\frac{\partial^2\theta}{\partial t^2}=0\\&\frac{\partial^2 P}{\partial x^2}-\frac{\partial Q}{\partial x}-q+I_0\frac{\partial^2 w}{\partial t^2}-I_1\frac{\partial^4 w}{\partial x^2\partial t^2}-I_2\frac{\partial^3\theta}{\partial x\partial t^2}-N\frac{\partial^2 w}{\partial x^2}+N_T\frac{\partial^2 w}{\partial x^2}=0\end{aligned} \tag{21}$$

where N in Eq. (21) is a constant. Moreover, certain general forces and moments of inertia involved with Eq. (21) are presented as

$$(N,P,M,Q)=\int_A\left(\sigma_x,\sigma_x f,\sigma_z g,\tau_{xy}\frac{\partial f}{\partial y}+\tau_{xz}\frac{\partial g}{\partial z}\right)\mathrm{d}A;(I_0,I_1,I_2,I_3)=\int_A\rho_f\left(1,f^2,fg,g^2\right)\mathrm{d}A$$

Combined with the nonlocal strain gradient constitutive relations, general forces of the tube are defined as

$$\begin{aligned}&N-\mu^2\frac{\partial^2 N}{\partial x^2}=A_1\left(1-l^2\nabla^2\right)\frac{1}{2}\left(\frac{\partial w}{\partial x}\right)^2-\left(1-l^2\nabla^2\right)N_T\\&P-\mu^2\frac{\partial^2 P}{\partial x^2}=A_3\left(1-l^2\nabla^2\right)\frac{\partial^2 w}{\partial x^2}+A_4\left(1-l^2\nabla^2\right)\frac{\partial\theta}{\partial x}\\&M-\mu^2\frac{\partial^2 M}{\partial x^2}=A_4\left(1-l^2\nabla^2\right)\frac{\partial^2 w}{\partial x^2}+A_5\left(1-l^2\nabla^2\right)\frac{\partial\theta}{\partial x}\\&Q-\mu^2\frac{\partial^2 Q}{\partial x^2}=A_7\left(1-l^2\nabla^2\right)\left(\frac{\partial w}{\partial x}+\theta\right)\end{aligned} \tag{22}$$

Other coefficients from Eq. (22) are given by

$$\left(A_1,A_3,A_4,A_5\right)=\int_A E_f\left(1,f^2,fg,g^2\right)\mathrm{d}A;A_7=\int_A G_f\left[\left(\frac{\partial f}{\partial y}\right)^2+\left(\frac{\partial g}{\partial z}\right)^2\right]\mathrm{d}A$$

For simply supported ends (S-S), necessary boundary conditions of the tube yield

$$X=0,L;u=0,w=0,M=0,P=0 \tag{23}$$

The governing equations of the tube proposed in Eq. (21) can be reformulated as

$$\begin{aligned}&A_3\frac{\partial^3 w}{\partial x^3}+A_5\frac{\partial^2\theta}{\partial x^2}-A_7\left(\frac{\partial w}{\partial x}+\theta\right)-l^2\left[A_4\frac{\partial^5 w}{\partial x^5}+A_5\frac{\partial^4\theta}{\partial x^4}-A_7\left(\frac{\partial^3 w}{\partial x^3}+\frac{\partial^2\theta}{\partial x^2}\right)\right]-I_2\frac{\partial^3 w}{\partial x\partial t^2}-I_3\frac{\partial^2\theta}{\partial t^2}\\&+\mu^2\left(I_2\frac{\partial^5 w}{\partial x^3\partial t^2}+I_3\frac{\partial^4\theta}{\partial x^2\partial t^2}\right)=0\end{aligned} \tag{24}$$

$$\begin{aligned}&A_3\frac{\partial^4 w}{\partial x^4}+A_4\frac{\partial^3\theta}{\partial x^3}-A_7\left(\frac{\partial^2 w}{\partial x^2}+\frac{\partial\theta}{\partial x}\right)-l^2\left[A_3\frac{\partial^6 w}{\partial x^6}+A_4\frac{\partial^5\theta}{\partial x^5}-A_7\left(\frac{\partial^4 w}{\partial x^4}+\frac{\partial^3\theta}{\partial x^3}\right)\right]-q-N\left(\frac{\partial^2 w}{\partial x^2}-\mu^2\frac{\partial^4 w}{\partial x^4}\right)\\&+N_T\left(\frac{\partial^2 w}{\partial x^2}-\mu^2\frac{\partial^4 w}{\partial x^4}\right)+I_0\frac{\partial^2 w}{\partial t^2}-I_1\frac{\partial^4 w}{\partial x^2\partial t^2}-I_2\frac{\partial^3\theta}{\partial x\partial t^2}-\mu^2\left(I_0\frac{\partial^4 w}{\partial t^2\partial x^2}-I_1\frac{\partial^6 w}{\partial x^4\partial t^2}-I_2\frac{\partial^5\theta}{\partial x^3\partial t^2}\right)=0\end{aligned} \tag{25}$$

in which the expression of N can be determined as

$$N=\frac{1}{L}\int_0^L\left[\frac{A_1}{2}\left(1-l^2\nabla^2\right)\left(\frac{\partial w}{\partial x}\right)^2\right]\mathrm{d}x-N_T$$

For the calculation convenience, introduce the following non-dimensional parameters.

$$\begin{aligned}&\bar{w}=\frac{w}{L};\xi=\frac{x}{L}\pi;\bar{\theta}=\frac{\theta}{\pi};S_0=\frac{I_0L^2E_0}{S\pi^2\rho_0};\left(S_1,S_2,S_3\right)=\frac{E_0}{S\rho_0}\left(I_1,I_2,I_3\right);\lambda_q=\frac{qL^3}{S\pi^4};S_n=\frac{\gamma_TL^2}{S\pi^2};\bar{\mu}=\frac{\mu\pi}{L};\\&\bar{l}=\frac{l\pi}{L};\lambda_T=\Delta T;\tau=\frac{\pi t}{L}\sqrt{\frac{E_0}{\rho_0}};\left(S_{11},S_{33},S_{44},S_{55},S_{77}\right)=\left(\frac{A_1L^2}{S\pi^2},\frac{A_3}{S},\frac{A_4}{S},\frac{A_5}{S},\frac{A_7L^2}{S\pi^2}\right);\end{aligned}$$

where

$$S=\int_A Ez^2\mathrm{d}A;\gamma_T=\int_A E_f\alpha_f\mathrm{d}A$$

General governing equations described in Eqs. (24), (25) can be rewritten as

$$\begin{aligned}&S_{44}\frac{\partial^3\bar{w}}{\partial\xi^3}+S_{55}\frac{\partial^2\bar{\theta}}{\partial\xi^2}-S_{77}\left(\frac{\partial\bar{w}}{\partial\xi}+\bar{\theta}\right)-\bar{l}^2\left[S_{44}\frac{\partial^5\bar{w}}{\partial\xi^5}+S_{55}\frac{\partial^4\bar{\theta}}{\partial\xi^4}-S_{77}\left(\frac{\partial^3\bar{w}}{\partial\xi^3}+\frac{\partial^2\bar{\theta}}{\partial\xi^2}\right)\right]-S_2\frac{\partial^3\bar{w}}{\partial\xi\partial\tau^2}\\&-S_3\frac{\partial^2\bar{\theta}}{\partial\tau^2}+\bar{\mu}^2\left(S_2\frac{\partial^5\bar{w}}{\partial\xi^3\partial\tau^2}+S_3\frac{\partial^4\bar{\theta}}{\partial\xi^2\partial\tau^2}\right)=0\end{aligned} \tag{26}$$

$$\begin{aligned}&S_{33}\frac{\partial^4\bar{w}}{\partial\xi^4}+S_{44}\frac{\partial^3\bar{\theta}}{\partial\xi^3}-S_{77}\left(\frac{\partial^2\bar{w}}{\partial\xi^2}+\frac{\partial\bar{\theta}}{\partial\xi}\right)-\bar{l}^2\left[S_{33}\frac{\partial^6\bar{w}}{\partial\xi^6}+S_{44}\frac{\partial^5\bar{\theta}}{\partial\xi^5}-S_{77}\left(\frac{\partial^4\bar{w}}{\partial\xi^4}+\frac{\partial^3\bar{\theta}}{\partial\xi^3}\right)\right]-\lambda_q\\&-\left\{\int_0^\tau\left[\frac{\pi S_{11}}{2}\left(\frac{\partial\bar{w}}{\partial\xi}\right)^2-\bar{l}^2S_{11}\pi\left(\frac{\partial\bar{w}}{\partial\xi}\cdot\frac{\partial^3\bar{w}}{\partial\xi^3}+\frac{\partial^2\bar{w}}{\partial\xi^2}\cdot\frac{\partial^2\bar{w}}{\partial\xi^2}\right)\right]\mathrm{d}\xi\right\}\left(\frac{\partial^2\bar{w}}{\partial\xi^2}-\bar{\mu}^2\frac{\partial^4\bar{w}}{\partial\xi^4}\right)+2S_n\lambda_T\left(\frac{\partial^2\bar{w}}{\partial\xi^2}-\bar{\mu}^2\frac{\partial^4\bar{w}}{\partial\xi^4}\right)\\&+S_0\frac{\partial^2\bar{w}}{\partial\tau^2}-S_1\frac{\partial^4\bar{w}}{\partial\xi^2\partial\tau^2}-S_2\frac{\partial^3\bar{\theta}}{\partial\xi\partial\tau^2}-\bar{\mu}^2\left(S_0\frac{\partial^4\bar{w}}{\partial\tau^2\partial\xi^2}-S_1\frac{\partial^6\bar{w}}{\partial\xi^4\partial\tau^2}-S_2\frac{\partial^5\bar{\theta}}{\partial\xi^3\partial\tau^2}\right)=0\end{aligned} \tag{27}$$

Meanwhile, the dimensionless boundary conditions can be described as

$$\overline{u}=0,\overline{w}=0,\overline{M}=0,\overline{P}=0;\ at\ \xi=0,\pi \tag{28}$$

4. Solution of the model

In this chapter, we obtain corresponding analytical solutions of Eqs. (26), (27) by using a two-steps perturbation procedure. To begin with, to get a set of vibration equations, we suppose that the expanded form of dimensionless displacement, dimensionless rotation angle and dimensionless transverse load can be expressed as

$$\begin{aligned}\overline{w}(\xi,\tau,\varepsilon)&=\sum_{n=1}\varepsilon^n w_n(\xi,\tau);\\ \overline{\theta}(\xi,\tau,\varepsilon)&=\sum_{n=1}\varepsilon^n \overline{\theta}_n(\xi,\tau);\\ \lambda_q(\xi,\tau,\varepsilon)&=\sum_{n=1}\varepsilon^n \lambda_n(\xi,\tau);\end{aligned}$$

where a small perturbation parameter(ε) has no physical meaning, which is introduced into Eqs. (26) and (27). Then, we collect terms of the same order(ε) to arrive at

$$\begin{aligned}&O(\varepsilon^1):\\ &S_{44}\frac{\partial^3\overline{w}_1}{\partial\xi^3}+S_{55}\frac{\partial^2\overline{\theta}_1}{\partial\xi^2}-S_{77}\left(\frac{\partial\overline{w}_1}{\partial\xi}+\overline{\theta}_1\right)-\overline{l}^2\left[S_{44}\frac{\partial^5\overline{w}_1}{\partial\xi^5}+S_{55}\frac{\partial^4\overline{\theta}_1}{\partial\xi^4}-S_{77}\left(\frac{\partial^3\overline{w}_1}{\partial\xi^3}+\frac{\partial^2\overline{\theta}_1}{\partial\xi^2}\right)\right]=0\end{aligned} \tag{29}$$

$$\begin{aligned}&S_{33}\frac{\partial^4\overline{w}_1}{\partial\xi^4}+S_{44}\frac{\partial^3\overline{\theta}_1}{\partial\xi^3}-S_{77}\left(\frac{\partial^2\overline{w}_1}{\partial\xi^2}+\frac{\partial\overline{\theta}_1}{\partial\xi}\right)-\overline{l}^2\left[S_{33}\frac{\partial^6\overline{w}_1}{\partial\xi^6}+S_{44}\frac{\partial^5\overline{\theta}_1}{\partial\xi^5}-S_{77}\left(\frac{\partial^4\overline{w}_1}{\partial\xi^4}+\frac{\partial^3\overline{\theta}_1}{\partial\xi^3}\right)\right]-\lambda_q^1\\ &+2S_n\lambda_T\left(\frac{\partial^2\overline{w}_1}{\partial\xi^2}-\overline{\mu}^2\frac{\partial^4\overline{w}_1}{\partial\xi^4}\right)=0\end{aligned} \tag{30}$$

$$\begin{aligned}&O(\varepsilon^3)\\ &S_{44}\frac{\partial^3\overline{w}_3}{\partial\xi^3}+S_{55}\frac{\partial^2\overline{\theta}_3}{\partial\xi^2}-S_{77}\left(\frac{\partial\overline{w}_3}{\partial\xi}+\overline{\theta}_3\right)-\overline{l}^2\left[S_{44}\frac{\partial^5\overline{w}_3}{\partial\xi^5}+S_{55}\frac{\partial^4\overline{\theta}_3}{\partial\xi^4}-S_{77}\left(\frac{\partial^3\overline{w}_3}{\partial\xi^3}+\frac{\partial^2\overline{\theta}_3}{\partial\xi^2}\right)\right]\\ &+\overline{\mu}^2\left(S_2\frac{\partial^5\overline{w}_1}{\partial\xi^3\partial\tau^2}+S_3\frac{\partial^4\overline{\theta}_1}{\partial\xi^2\partial\tau^2}\right)-S_2\frac{\partial^3\overline{w}_1}{\partial\xi\partial\tau^2}-S_3\frac{\partial^2\overline{\theta}_1}{\partial\tau^2}=0\end{aligned} \tag{31}$$

$$\begin{aligned}&S_{33}\frac{\partial^4\overline{w}_3}{\partial\xi^4}+S_{44}\frac{\partial^3\overline{\theta}_3}{\partial\xi^3}-S_{77}\left(\frac{\partial^2\overline{w}_3}{\partial\xi^2}+\frac{\partial\overline{\theta}_3}{\partial\xi}\right)-\overline{l}^2\left[S_{33}\frac{\partial^6\overline{w}_3}{\partial\xi^6}+S_{44}\frac{\partial^5\overline{\theta}_3}{\partial\xi^5}-S_{77}\left(\frac{\partial^4\overline{w}_3}{\partial\xi^4}+\frac{\partial^3\overline{\theta}_3}{\partial\xi^3}\right)\right]-\lambda_q^3\\ &-\left\{\int_0^\pi\left[\frac{\pi S_{11}}{2}\left(\frac{\partial\overline{w}_1}{\partial\xi}\right)^2-\overline{l}^2S_{11}\pi\left(\frac{\partial\overline{w}_1}{\partial\xi}\cdot\frac{\partial^3\overline{w}_1}{\partial\xi^3}+\frac{\partial^2\overline{w}_1}{\partial\xi^2}\cdot\frac{\partial^2\overline{w}_1}{\partial\xi^2}\right)\right]\mathrm{d}\xi\right\}\left(\frac{\partial^2\overline{w}_1}{\partial\xi^2}-\overline{\mu}^2\frac{\partial^4\overline{w}_1}{\partial\xi^4}\right)\\ &+S_0\frac{\partial^2\overline{w}_1}{\partial\tau^2}-S_1\frac{\partial^4\overline{w}_1}{\partial\xi^2\partial\tau^2}-S_2\frac{\partial^3\overline{\theta}_1}{\partial\xi\partial\tau^2}-\overline{\mu}^2\left(S_0\frac{\partial^4\overline{w}_1}{\partial\tau^2\partial\xi^2}-S_1\frac{\partial^6\overline{w}_1}{\partial\xi^4\partial\tau^2}-S_2\frac{\partial^5\overline{\theta}_1}{\partial\xi^3\partial\tau^2}\right)\\ &+2S_n\lambda_T\left(\frac{\partial^2\overline{w}_3}{\partial\xi^2}-\overline{\mu}^2\frac{\partial^4\overline{w}_3}{\partial\xi^4}\right)=0\end{aligned} \tag{32}$$

To solve respective differential perturbation equations, asymptotic solutions of dimensionless displacement as well as dimensionless rotation angle, satisfying simply supported ends, are given by

$$\begin{aligned}\overline{w}(\xi,\tau)&=\varepsilon A_{10}^1\sin(m\xi)+O(\varepsilon^4);\\ \overline{\theta}(\xi,\tau)&=\varepsilon B_{10}^1\cos(m\xi)+\varepsilon^3B_{10}^3\cos(m\xi)+O(\varepsilon^4);\end{aligned} \tag{33}$$

Submitting Eq. (33) into Eq. (29), we could have

$$B_{10}^1=-\frac{S_{44}m^3+S_{77}m}{S_{55}m^2+S_{77}}A_{10}^1 \tag{34}$$

By submitting Eqs. (33) and (34) into Eq. (30), λ_q^1 is determined in the following form.

$$\lambda_q^1=\left\{m^4\left(1+m^2\overline{l}^2\right)\left[S_{33}-\frac{S_{44}\left(S_{44}m^2+S_{77}\right)}{S_{55}m^2+S_{77}}-\frac{S_{77}\left(S_{44}-S_{55}\right)}{S_{55}m^2+S_{77}}\right]-2S_n\lambda_Tm^2\left(1+\overline{\mu}^2m^2\right)\right\}A_{10}^1\sin(m\xi) \tag{35}$$

Later on, the substitution of Eq. (33) and Eq. (34) into Eq. (31), one has

$$B_{10}^3=\left[\frac{S_3\left(S_{44}m^3+S_{77}m\right)}{\left(S_{55}m^2+S_{77}\right)^2}-\frac{S_2m}{S_{55}m^2+S_{77}}\right]\frac{\left(1+m^2\overline{\mu}^2\right)}{\left(1+m^2\overline{l}^2\right)}\ddot{A}_{10}^1 \tag{36}$$

λ_q^3 is determined by submitting Eq. (33), (34) and (36) into Eq. (32)

$$\begin{aligned}\lambda_q^3=&\left[S_1m^2+S_0+\frac{S_3\left(S_{44}m^3+mS_{77}\right)^2}{\left(S_{55}m^2+S_{77}\right)^2}-\frac{2S_2m^2\left(S_{44}m^2+S_{77}\right)}{\left(S_{55}m^2+S_{77}\right)}\right]\ddot{A}_{10}^1\left(1+m^2\overline{\mu}^2\right)\sin(m\xi)\\ &+\frac{\pi^2S_{11}m^4}{4}\left(A_{10}^1\right)^3\left(1+m^2\overline{\mu}^2\right)\sin(m\xi)\end{aligned} \tag{37}$$

Eventually, the analytical solution of non-dimension transverse load can be expressed as

$$\lambda_q=\lambda_q^1+\lambda_q^3+O\left(\varepsilon^4\right) \tag{38}$$

Because the value of λ_q is equivalent to zero when solving free vibration problems, we apply the method of Galerkin to Eq. (38), obtaining the Duffing equation.

$$J_{30}\frac{\mathrm{d}^2\left(\varepsilon A_{10}^1\right)}{\mathrm{d}t^2}+J_{31}\left(\varepsilon A_{10}^1\right)+J_{33}\left(\varepsilon A_{10}^1\right)^3=0 \tag{39}$$

where

$$J_{30}=\left[S_1m^2+S_0+\frac{S_3\left(S_{44}m^3+mS_{77}\right)^2}{\left(S_{55}m^2+S_{77}\right)^2}-\frac{2S_2m^2\left(S_{44}m^2+S_{77}\right)}{\left(S_{55}m^2+S_{77}\right)}\right]\left(1+m^2\overline{\mu}^2\right)$$

$$J_{31}=m^4\left(1+m^2\overline{l}^2\right)\left[S_{33}-\frac{S_{44}\left(S_{44}m^2+S_{77}\right)}{S_{55}m^2+S_{77}}-\frac{S_{77}\left(S_{44}-S_{55}\right)}{S_{55}m^2+S_{77}}\right]-2S_n\lambda_Tm^2\left(1+\overline{\mu}^2m^2\right)$$

$$J_{33}=\frac{\pi^2S_{11}m^4}{4}\left(1+m^2\overline{\mu}^2\right)$$

So, the analytical solution of Eq. (39) can be written as

$$\omega_{NL}=\omega_L\sqrt{1+\frac{3J_{33}}{4J_{31}}\left(A_{10}^1\right)^2};\omega_L=\sqrt{\frac{J_{31}}{J_{30}}};$$

where the symbol of A_{10}^1 ($A_{10}^1=W_m/L$) is dimensionless amplitude of the tube. ω_L and ω_{NL} stand for dimensionless linear frequency and dimensionless nonlinear frequency, respectively.

So far, the majority of theoretical models have been established based on three classical theories. They are Euler beam model, Timoshenko beam model as well as Reddy beam model. In the following part, three classical beam models are derived from the present model.

When *f*=-*z*, the displacement function Eq. (11) can be converted to Euler-Bernoulli model. Corresponding coefficients are

Table 1 Temperature-dependent coefficients of material properties (Reddy and Chin 1998)

Material	Properties	P_0	P_{-1}	P_1	P_2	P_3
Si_3N_4	E(Pa)	$348.43\times10^{+9}$	0.0	-3.070×10^{-4}	2.160×10^{-7}	-8.964×10^{-11}
	α(1/k)	5.8723×10^{-6}	0.0	9.095×10^{-4}	0.0	0.0
	p(Kg/m^3)	2370	0.0	0.0	0.0	0.0
	v	0.24	0.0	0.0	0.0	0.0
SUS304	E(Pa)	$201.04\times10^{+9}$	0.0	3.079×10^{-4}	-6.543×10^{-7}	0.0
	α(1/k)	12.33×10^{-6}	0.0	8.096×10^{-4}	0.0	0.0
	p(Kg/m^3)	8166	0.0	0.0	0.0	0.0
	v	0.3262	0.0	0.0	0.0	0.0

$$J_{30}=\left(S_0+S_1m^2\right)\left(1+m^2\bar{\mu}^2\right);\ J_{31}=m^4\left(1+m^2\bar{l}^2\right)S_{33}-2S_n\lambda_T m^2\left(1+m^2\bar{\mu}^2\right);\ J_{33}=\frac{\pi^2S_{11}m^4}{4}\left(1+m^2\bar{\mu}^2\right);\tag{40}$$

When f=0, the displacement function Eq. (11) can be converted to Timoshenko model. Corresponding coefficients are

$$J_{30}=\left(1+m^2\bar{\mu}^2\right)\left[S_0+\frac{m^2S_3\left(S_{77}k_s\right)^2}{\left(S_{55}m^2+k_sS_{77}\right)^2}\right];\ J_{31}=\frac{m^4S_{55}S_{77}k_s}{m^2S_{55}+S_{77}k_s}\left(1+m^2\bar{l}^2\right)-2S_n\lambda_T m^2\left(1+m^2\bar{\mu}^2\right);\ J_{33}=\frac{\pi^2S_{11}m^4}{4}\left(1+m^2\bar{\mu}^2\right)\tag{41}$$

where the shear factor k_s of Eq. (41) is from Zhang and Fu (2013).

$$k_s=\frac{6\left(\bar{R}_i^2+1\right)^2\left(1+v\right)^2}{\left(7+12v+4v^2\right)\left(\bar{R}_i^4+1\right)+\left(34+48v+16v^2\right)\bar{R}_i^2}$$

in which $\bar{R}_i=R_i/R_0$ and the Poisson's ratio v is considered to be the average value of two materials.

When $f=-4z^3/\left(3h^2\right)$, the displacement function Eq. (11) can be converted to Reddy model. Corresponding coefficients are the same with ones of the present model. More detailed information can be found from Eq. (39).

5. Results and discussions

In this part, we fully utilize above analytical solutions to investigate functionally graded nano-tubes. Based on results obtained, some new findings are revealed, which are different from what are predicted from the conventional theories and models.

5.1 Validation research

Before discussions of respective physical parameters, both dimensionless free vibration frequencies of functionally graded rod and non-dimension frequencies of isotropic tube are calculated by present mathematical model, which can verify the present deduced results directly. In Table 2, the dimensionless frequency of a functionally graded rod with (R_i=0, L=10R_0, T=300K,) is used to verify the current solution. When R_i=0, the present shear deformation beam model can still satisfy necessary stress boundary conditions on the surface of circular cylindrical rods. This table to demonstrate a small difference between those results reported by Shen and Wang (2014) and Huang *et al.* (2010) and ones in this study clearly indicates that present solution is reliable and reasonable. To further validate the present analysis, the dimensionless natural frequency for an isotropic cylindrical shell with (R_i=0.998R_0, L=20R_0, v=0.3, T=300K) under simply supported ends are tabulated in Table 3. As we all see from Table 3, present results produced by the model show a good agreement with published ones. Therefore, the two examples amply demonstrate the validation of the present analysis and solution for nonlinear vibration problem.

Table 2 Comparisons of non-dimension natural frequencies ($\omega=\Omega R\sqrt{\rho_c/G_c}$) of FGM circular cylindrical beams

N	Source	ω_1	ω_2	ω_3	ω_4	ω_5	ω_6
1	Present	0.0901817	0.317009	0.613347	0.940205	1.27975	1.62443
	Shen and Wang (2014)	0.09	0.3175	0.6159	0.9462	1.29	1.6394
	difference	0.2019%	0.1546%	0.4145%	0.6336%	0.7946%	0.9131%
	Huang *et al.* (2010)	0.0902	0.3193	0.617	0.9459	1.2867	1.6311
	difference	0.0203%	0.7175%	0.5921%	0.6021%	0.5401%	0.4089%
5	Present	0.0882979	0.308939	0.595295	0.909696	1.23538	1.56546
	Shen and Wang (2014)	0.0883	0.3089	0.5953	0.9097	1.2353	1.5654
	difference	0.0024%	0.0126%	0.0008%	0.0004%	0.0065%	0.0038%
	Huang *et al.* (2010)	0.0885	0.3095	0.5954	0.9075	1.2291	1.5531
	difference	0.2284%	0.1813%	0.0176%	0.2420%	0.5109%	0.7958%

Table 3 Comparisons of non-dimension natural frequencies ($\omega=\Omega R_0\sqrt{(1-v^2)\rho/E}$) of an isotropic cylindrical shell

Source	ω_1	ω_2	ω_3	ω_4	ω_5	ω_6
Present	0.016032	0.0584366	0.116619	0.182637	0.252086	0.322774
Huang *et al.* (2010)	0.016	0.0583	0.1166	0.1827	—	—
difference	0.2000%	0.2343%	0.0163%	0.0345%	—	—
Zhang *et al.* (2001)	0.0161065	—	—	—	—	—
difference	0.4625%	—	—	—	—	—

5.2 Discussions of physical parameters

Before starting the discussions of respective physical parameters, something important must be presented. The formulation of the non-dimension frequency is $\omega=\Omega\left(L^2/R_0\right)\sqrt{\rho_0/E_0}$ where $\Omega=\omega_L\left(\pi/L\right)\sqrt{E_0/\rho_0}$ .The values of ρ_0 and E_0 are equivalent to 8166 kg/m^3 and 201.04 GPa, respectively. The effective properties of two types of material (SUS304, Si_3N_4) are tabulated in Table 1.

Within the results of Table 4, the effect of slenderness ratio, scale parameter ratio and respective beam models on

Table 4 Comparisons of different beam models and scale parameter ratio on non-dimension natural frequency for the tube. (N=1, T=300K, μ=1nm, R_i=0.8R_0, R_0=1 nm)

Ratio	Type	L=10R_0	L=20R_0	L=30R_0	L=40R_0	L=50R_0	L=60R_0	L=70R_0	L=80R_0
l=0.5μ	Present	8.01729	8.88595	9.07549	9.14449	9.17689	9.19461	9.20535	9.21233
	Reddy	8.498	9.03555	9.14509	9.18425	9.20253	9.21249	9.21852	9.22243
	Timoshenko	8.08813	8.90948	9.08664	9.15087	9.18101	9.19749	9.20747	9.21396
	Euler	8.75055	9.1074	9.17784	9.20284	9.21447	9.22081	9.22463	9.22712
l=μ	Present	8.30182	8.96729	9.07299	9.11268	9.16559	9.19045	9.20429	9.21299	9.21766
	Reddy	8.7996	9.11826	9.18252	9.20544	9.21613	9.22195	9.22547	9.22776
	Timoshenko	8.37518	8.89104	9.04982	9.12382	9.17198	9.19464	9.20742	9.21442	9.21928
	Euler	9.06111	9.19077	9.2154	9.22407	9.22809	9.23027	9.23159	9.23245
l=1.5μ	Present	8.75552	9.10125	9.12592	9.17425	9.19501	9.20577	9.21386	9.22652
	Reddy	9.2805	9.25447	9.24456	9.24065	9.23875	9.2377	9.23706	9.23664
	Timoshenko	8.83288	9.12535	9.18547	9.20706	9.21715	9.22266	9.22599	9.22815
	Euler	9.5563	9.32807	9.27767	9.25935	9.25074	9.24603	9.24318	9.24133

Table 5 Effect of nonlocal parameter μ on non-dimension natural frequency for the tube. (R_i=0.8R_0, R_0=1 nm, T=300K, L=20R_0, N=1, l=0)

ω	μ=0	μ=1nm	μ=2nm	μ=4nm	μ=6nm	μ=8nm	μ=10nm
ω_1	8.96729	8.85867	8.55505	7.5929	6.52574	5.58373	4.8157
ω_2	33.2073	31.6807	28.1177	20.6774	15.5626	12.2767	10.0723
ω_3	67.4045	60.9735	49.0521	31.5891	22.4752	17.2819	13.9921
ω_4	107.132	90.7119	66.7084	39.6063	27.4676	20.9035	16.8386

Table 6 Effect of strain gradient parameter l on non-dimension natural frequency for the tube. (R_i=0.8R_0, R_0=1 nm, T=300K, L=20R_0, N=1, μ=0)

ω	l=0	l=1nm	l=2nm	l=4nm	l=6nm	l=8nm	l=10nm
ω_1	8.96729	9.07725	9.3994	10.5905	12.3223	14.4012	16.698
ω_2	33.2073	34.8074	39.2181	53.3299	70.8574	89.8228	109.481
ω_3	67.4045	74.5137	92.6233	143.827	202.15	262.897	324.709
ω_4	107.132	126.523	172.05	289.781	417.844	549.055	681.6

non-dimension natural frequency for the tube can be illustrated as follows:

(i) The present model on non-dimension natural frequencies for the tube is similar to the model of Timoshenko, but smaller than Reddy model and Euler model. Besides, these results explicitly indicate that transverse shear deformation plays an important role in short FGM tubes, thus the frequencies obtained by the Euler beam model are higher than those obtained by others.

(ii) When scale parameter ratio (l/μ) continues to rise, the dimensionless frequency of the tube has an increasing trend, remarkably. So, scale parameter ratio cannot be ignored in analysis of nano-structure.

(iii) A higher slenderness ratio tends to weaken the stiffness of the tube. That is to say: with the slenderness ratio becoming large, the frequency continues to ascend, regardless of which model is adopted. When L=60R_0, the results obtained by four types of beam model are almost the same.

Table 7 Effect of dimensionless temperature λ_T on non-dimension natural frequency for the tube. (R_i=0.8R_0, R_0=1 nm, L=20R_0, N=1, μ=1 nm)

Ratio	ω	λ_T=0	λ_T=50	λ_T=100	λ_T=150	λ_T=200	λ_T=250
l=0.5μ	ω_1	8.88595	8.30679	7.65315	6.90711	6.03859	4.98946
	ω_2	32.0692	31.3511	30.5774	29.7459	28.8546	27.9009
	ω_3	62.6432	61.7119	60.7121	59.6424	58.5013	57.2875
	ω_4	95.083	93.8989	92.6266	91.2642	89.8099	88.2622
l=μ	ω_1	8.96729	8.39298	7.74572	7.00848	6.15298	5.12564
	ω_2	33.2073	32.5042	31.7473	30.9349	30.0651	29.1359
	ω_3	67.4045	66.4984	65.526	64.486	63.3771	62.1981
	ω_4	107.132	105.979	104.741	103.414	101.997	100.488
l=1.5μ	ω_1	9.10125	8.53469	7.8976	7.17425	6.33905	5.3449
	ω_2	35.0221	34.3401	33.6069	32.8211	31.981	31.0852
	ω_3	74.6683	73.789	72.8456	71.8366	70.7607	69.6168
	ω_4	124.651	123.515	122.293	120.982	119.58	118.084

Table 5 shows the effect of nonlocal parameter μ on non-dimension natural frequency for the tube. It can be observed from this table that the frequency is getting smaller when the value of parameter μ becomes larger and other size parameters remain unchanged. Hence, we have demonstrated the non-local parameter μ has a tendency to reduce the non-dimension natural frequencies of the tube. Table 6 shows the effect of strain gradient parameter l on non-dimension natural frequency for the tube. As can be seen from the table, the frequency is getting bigger when the value of strain gradient parameter l becomes larger and other size parameters remain unchanged. Thus, in contrast to the effect of nonlocal parameter μ, strain gradient parameter l increases the non-dimension natural frequency for the tube. From what has been analyzed above, nonlocal parameter μ and strain gradient parameter l have the opposite effect on the natural frequency of nano-tubes.

Fig. 3 presents variation of the natural frequency relevant to the scale parameter ratio(l/μ) for functionally graded nanotubes. It can be seen from this figure that the results from nonlocal strain gradient theory are equivalent to those from classical elasticity theory when l=μ. This equivalence relation can be predicted from Eq. (35), Eq. (36) and Eq. (39). The reason is that the scale parameter ratio (l/μ=1) can result in the Eq. (35) and Eq. (36) degenerating the equations of classical model, then nonlocal parameter μ and strain gradient parameter l can't be contained in the Duffing equation, namely Eq. (39). Consequently, the present model established by nonlocal strain gradient theory is identical with the model obtained by classical elasticity theory. As described in this figure, when l/μ<1, the frequencies obtained by nonlocal strain gradient theory are all smaller than those obtained by classical elasticity theory. Also, the frequencies can be obviously reduced with the rise of nonlocal parameter μ. Nevertheless, when l/μ>1, the frequencies obtained by nonlocal strain gradient theory are all bigger than those obtained by classical elasticity theory. Additionally, the

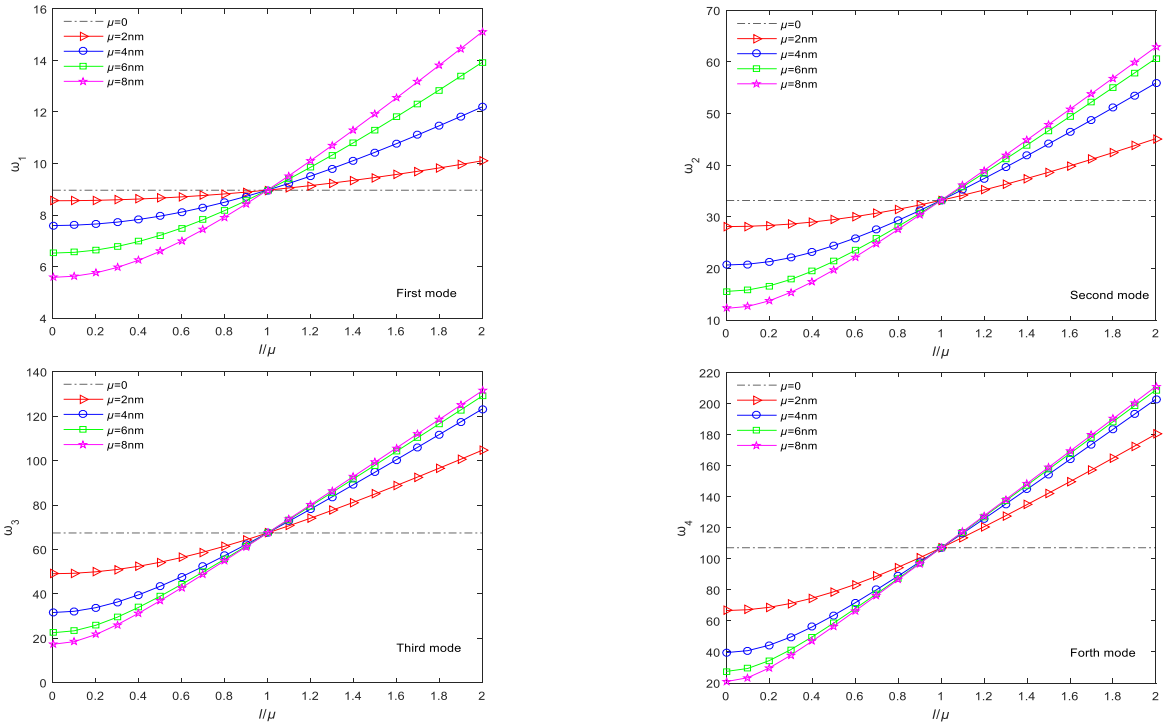

Fig. 3 Variation of the natural frequency relevant to l/μ for the nanotube (R_i=0.8R_0, R_0=1nm, T=300K, L=20R_0, N=1)

Table 8 Effect of inner radius R_i to outer radius R_0 ratio on non-dimension natural frequency for the tube. (T=300k, R_0=1 nm, μ=1 nm, L=20R_0, N=1)

Ratio	ω	R_i=0	R_i=0.2R_0	R_i=0.4R_0	R_i=0.6R_0	R_i=0.8R_0	R_i=0.99R_0
l=0.5μ	ω_1	8.12123	7.90076	8.01052	8.36055	8.88595	9.50184
	ω_2	30.5843	29.6267	29.7335	30.6183	32.0692	33.815
	ω_3	62.9111	60.6014	60.0422	60.8269	62.6432	65.068
	ω_4	100.391	96.1521	94.0532	93.7851	95.083	97.4799
l=μ	ω_1	8.19557	7.97309	8.08385	8.43709	8.96729	9.58882
	ω_2	31.6697	30.6782	30.7888	31.705	33.2073	35.0151
	ω_3	67.6927	65.2075	64.6058	65.4501	67.4045	70.0136
	ω_4	113.113	108.336	105.971	105.669	107.132	109.832
l=1.5μ	ω_1	8.318	8.09219	8.20461	8.56312	9.10125	9.73206
	ω_2	33.4005	32.3547	32.4714	33.4377	35.0221	36.9287
	ω_3	74.9876	72.2346	71.568	72.5033	74.6683	77.5586
	ω_4	131.61	126.052	123.301	122.949	124.651	127.793

Table 9 Effect of volume indexes N on non-dimension natural frequency for the tube. (R_i=0.8R_0, R_0=1 nm, L=20R_0, T=300K, μ=1 nm)

Ratio	ω	N=0	N=1	N=2	N=3	N=4	N=5
l=0.5μ	ω_1	14.303	8.88595	7.86259	7.40958	7.15111	6.98327
	ω_2	51.7238	32.0692	28.3567	26.7154	25.7798	25.1726
	ω_3	101.264	62.6432	55.3496	52.1289	50.295	49.1058
	ω_4	154.018	95.083	83.9552	79.0471	76.2546	74.4448
l=μ	ω_1	14.4339	8.96729	7.9345	7.4774	7.21658	7.0472
	ω_2	53.5595	33.2073	29.3631	27.6635	26.6947	26.066
	ω_3	108.961	67.4045	59.5565	56.091	54.1177	52.8381
	ω_4	173.534	107.132	94.5937	89.0637	85.9173	83.8782
l=1.5μ	ω_1	14.6495	9.10125	8.05309	7.5891	7.32438	7.15247
	ω_2	56.4865	35.0221	30.9678	29.1753	28.1536	27.4905
	ω_3	120.703	74.6683	65.9745	62.1357	59.9497	58.5322
	ω_4	201.912	124.651	110.063	103.628	99.9674	97.5949

frequencies can be increased with the value of nonlocal parameter μ becoming big. From what has been discussed above, the natural frequency predicted by nonlocal strain gradient theory is determined by nonlocal parameter, strain gradient parameter and the strain gradient parameter to nonlocal parameter ratio, together. In addition, It can be found from this figure that the size effect is more notable for higher-order frequencies.

It can be calculated from Eq. (35) and Eq. (39) that when the value of dimensionless temperature λ_T becomes large, the result of ω_L will descend. As we predict, the results of Table 7 indicate that with the non-dimension temperature elevating, the dimensionless frequencies of the tube subjected to uniform thermal environment diminish, continuously. Besides, as the scale parameter ratio (l/μ) continues to increase, the dimensionless frequency is getting bigger and bigger.

Due to demands of tubes with different radius in engineering, the effect of inner radius R_i to outer radius R_0 ratio on non-dimension natural frequencies of the tube has been investigated in Table 8. It can be revealed from the above that as the thickness of the tube continues to reduce, the dimensionless natural frequencies of the tube decrease at first, then remarkably increase. In terms of this trait, the thickness of the tube should be taken into account in design of tubes.

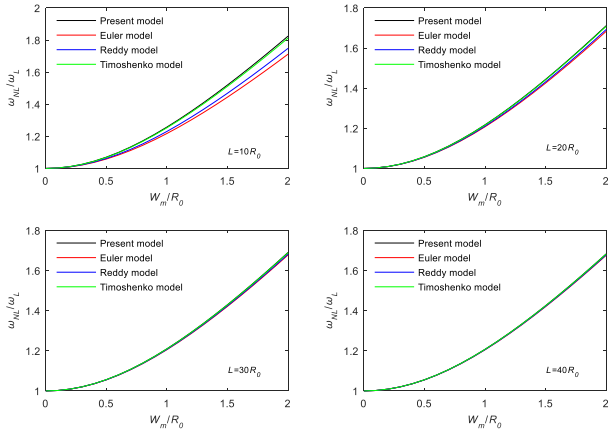

Fig. 4 Comparisons of different beam models on the amplitude-frequency of the tube. (R_i=0.8R_0, R_0=1 nm, T=300K, μ=1 nm, N=1, l=0.5μ)

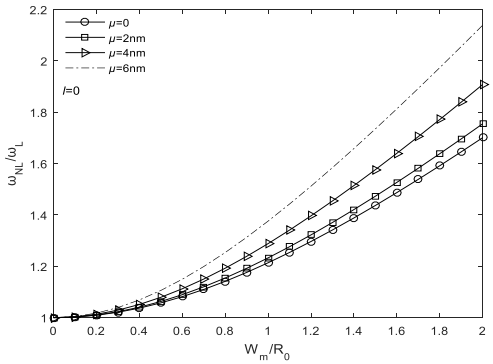

Fig. 5 The effect of non-local parameter μ relevant to the amplitude-frequency of the tube. (R_0=1 nm, T=300K, R_i=0.8R_0, L=20R_0, N=1, l=0)

Results from Table 9 distinctly reflects the influence of material volume indexes N on non-dimension natural frequency for the tube. That is, when increasing the content of SUS304, dimensionless natural frequency of the tube is going to decline, continuously.

Fig. 4 presents comparisons of different beam models on the amplitude-frequency of the tube. In this figure, W_m/R_0 symbolizes the non-dimension amplitude of nonlinear vibration; And, ω_{NL}/ω_L represents frequency ratio which is equal to the value of the nonlinear frequency divided by corresponding linear frequency. It can be seen from this figure that the results of present model is higher than other beam model and the results of Euler beam model is the lowest when L=10R_0. However, with the increment of slenderness ratio, respective results begin to be nearly the same. So, we can know that transverse shear plays a crucial role in short tubes, whereas it can be neglected for long enough tubes.

Fig. 5 depicts the effect of non-local parameter μ with respective to the amplitude-frequency of the tube. These curves from the figure reveal that the nonlinear frequency to linear frequency ratio of the FGM tube can be remarkably improved by increasing the value of nonlocal parameter μ. So, the small scale parameter μ has an indispensable role in the nonlinear vibration problem.

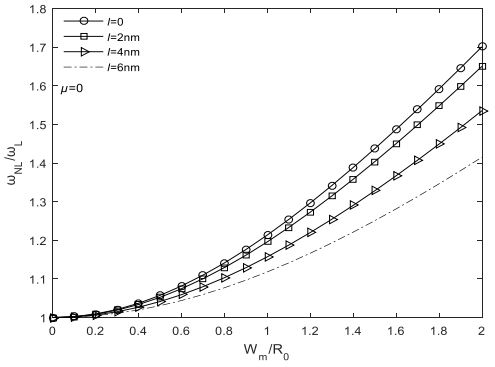

Fig. 6 The effect of strain gradient parameter l relevant to the amplitude-frequency of the tube. (R_0=1 nm, T=300K, R_i=0.8R_0, L=20R_0, N=1, μ=0)

Fig. 6 shows the effect of strain gradient parameter l relevant to the amplitude-frequency of the tube. Comparing with the effect of non-local parameter μ, a gradual increasing material length scale parameter l can reduce the nonlinear frequency to linear frequency ratio of the FGM tubes, remarkably. Thus, we could know that nonlocal parameter μ and strain gradient parameter l have the opposite effect on the nonlinear vibration problem.

Fig. 7 exhibits the variation of nonlinear to linear frequency of the tube relevant to relevant to l/μ for functionally graded nanotubes. Obviously, when l=μ, the frequency ratio obtained by nonlocal strain gradient theory is identical with the classical frequency ratio. When l/μ<1, the frequency ratio obtained by the present model is higher than that of classical continuum model; and the nonlinear frequency is remarkably increased with the rise of nonlocal parameter μ. But, when l/μ>1, the frequency ratio obtained by the present model is smaller than that of classical continuum model; and the nonlinear frequency is remarkably decreased with the rise of nonlocal parameter μ. So, the variation trend of the nonlinear frequency is different from that of linear frequency when the scale parameter ratio l/μ is changed and other parameters remain unchanged. The reason can be found from its analytical solution. Throughout analyzing the expression of ω_{NL}, we could have a good knowledge that the effect of stiffness-hardening, namely the strain gradient theory, on the nonlinear vibration frequency is bigger than the effect of stiffness-softening, namely the nonlocal elasticity theory, on the nonlinear vibration frequency at a comparatively smaller value of the parameter l, whereas, is smaller than the effect of stiffness-softening on the nonlinear vibration frequency at a comparatively larger value of the parameter l. The effects of stiffness-softening and stiffness-hardening cancel each other out when both values of l and μ are equal, which is similar to classical continuum model. Besides, it can be seen that the nonlinear frequencies with W_m/R_0=3 is greater than ones with W_m/R_0=1. That is the nonlinear vibration frequency varies along dimensionless vibration amplitude, different from the linear frequency. The attribute of nonlinear vibration is just like hardening spring behaviors.

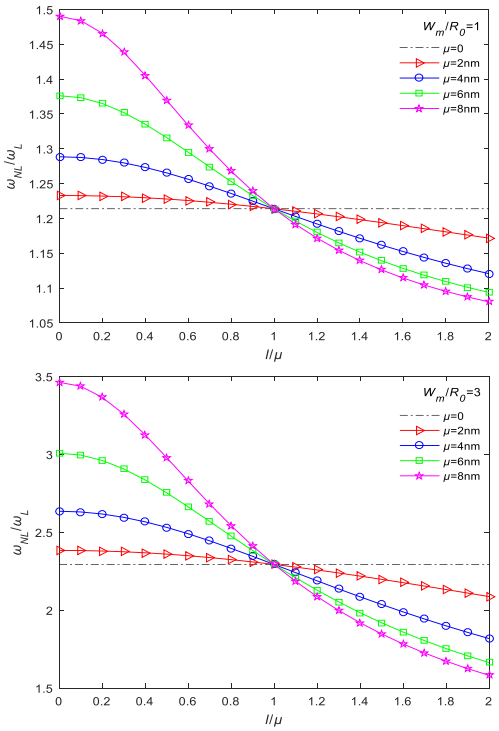

Fig. 7 Comparison of nonlinear to linear frequency of the tube relevant to relevant to l/μ for different nonlocal parameters. (R_0=1 nm, T=300K, R_i=0.8R_0, L=20R_0, N=1)

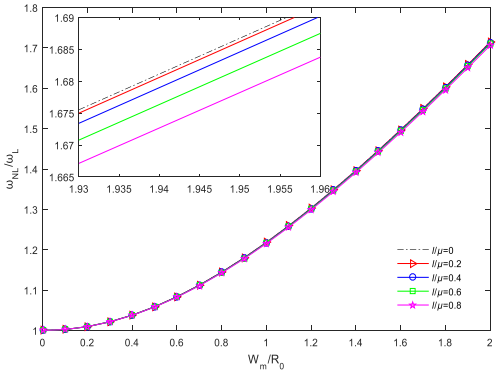

Fig. 8 The influence of l/μ relevant to the amplitude-frequency of the tube. (R_0=1 nm, R_i=0.8R_0, L=20R_0, N=1, μ=1 nm, T=300K)

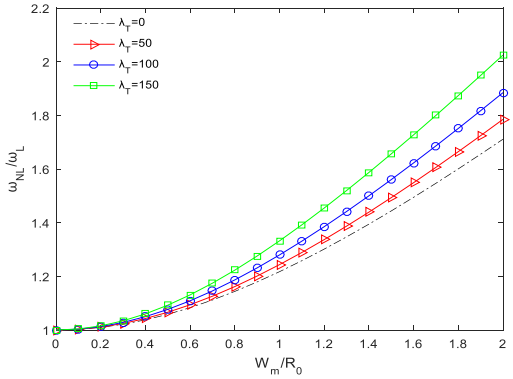

Fig. 9 The influence of dimensionless temperature λ_T relevant to the amplitude-frequency of the tube. (R_0=1 nm, R_i=0.8R_0, L=20R_0, N=1, μ=1 nm, l=0.5μ)

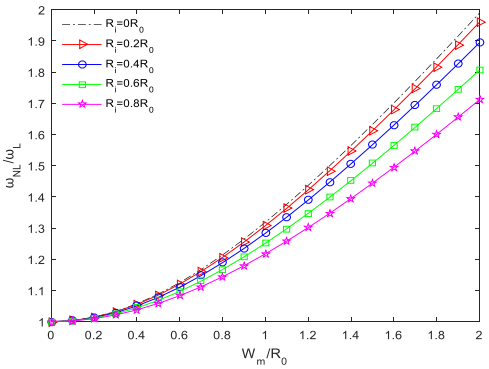

Fig. 10 The influence of inner radius R_i above the amplitude frequency of the tube. (R_0=1 nm, T=300K, L=20R_0, N=1, μ=1 nm, l=0.5μ)

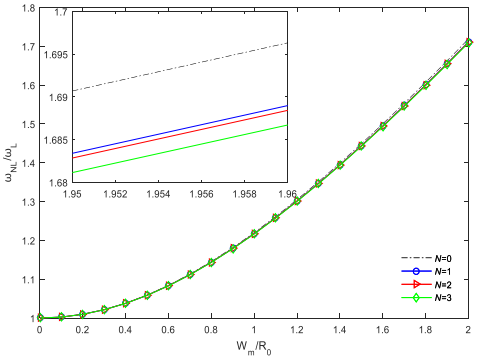

Fig. 11 The influence of material index N relevant to the frequency of the tube. (R_0=1 nm, T=300K, L=20R_0, R_i=0.8R_0, μ=1 nm, l=0.5μ)

Fig. 8 describes the influence of l/μ relevant to the amplitude-frequency of the tube. From this figure, the phenomenon can be observed that the nonlinear frequency to linear frequency ratio can be reduced with the rise of the value of the scale parameter ratio (l/μ). Combined with the results of Tables 7-9, a conclusion can be drawn that as the scale parameter ratio (l/μ) continues to increase, the dimensionless linear frequency is getting bigger and bigger while the dimensionless nonlinear frequency is becoming smaller and smaller.

Fig. 9 presents the effect of non-dimension temperature relevant to the amplitude-frequency of the tube. It can be found from this figure that the nonlinear frequency to linear frequency ratio will be definitely increased when the tube is exposed to a rising thermal environment. The results of Fig. 10 can be predicted from Eqs. (35) and (39). The reason is that a higher dimensionless temperature λ_T can lead to the denominator of the expression of ω_{NL}/ω_L becoming smaller.

Fig. 10 describes the influence of inner radius R_i above the amplitude frequency of the tube. It can be seen that when taking larger inner radius under the same outer radius, the nonlinear to linear frequencies ratio goes down.

Fig. 11 shows the influence of material index N with respective to the amplitude-frequency of the tube. From this figure, a conclusion can be drawn that with material indexes N increasing, corresponding amplitude frequency curves become lower. In other words, as the content of SUS304

continues to ascend, the nonlinear vibration frequencies are going to reduce, gradually.

6. Conclusions

This paper analyzes free vibration of functionally graded nano-tubes by using nonlocal strain gradient theory and a refined beam model. The refined beam model can satisfy the shear stress boundary conditions, which can degenerate the Euler beam model, the Timoshenko beam model and the Reddy beam model. Then, the nonlinear vibration model is established with the aid of Hamilton's principle. By using a two-steps perturbation method, the analytical solution is obtained to carry out a vibration analysis in detail. Finally, some important conclusions are outlined.

(1) Shown by comparison among different beam models, the transverse shear deformation will play a crucial role on nonlinear and linear frequencies if nanotubes are relatively short, but it can be neglected if nanotubes are relatively long.

(2) The rise of nonlocal parameter μ and the descend of strain gradient parameter l can reduce the linear vibration frequency but increase the nonlinear vibration frequency.

(3) Compared with classical frequencies, the linear and nonlinear frequencies from the nonlocal strain gradient theory may be smaller, the same or bigger, which is determined by strain gradient parameter, nonlocal parameter and the strain gradient parameter to nonlocal parameter ratio, together.

(4) The decrease of the thickness of tubes make the linear frequencies small, firstly, then grow, but make the nonlinear to linear frequency ratio small all the while.

(5) The increase of dimensionless temperature can reduce the linear frequency, however, improve the nonlinear to linear frequency ratio.

(6) The linear and nonlinear frequencies can be decreased with the increment of volume index(N).

The above-obtained conclusions can provide theoretical references for optimization designs of structures made of FGMs under thermal environments. Moreover, they are also immensely useful for others undertaking the analysis of nano-materials.

References

Abdelaziz, H.H., Meziane, M.A.A., Bousahla, A.A., Tounsi, A., Mahmoud, S.R. and Alwabli, A.S. (2017), "An efficient hyperbolic shear deformation theory for bending, buckling and free vibration of fgm sand wich plates with various boundary conditions", *Steel Compos. Struct.*, **25**(6), 693-704.

Ahmed, H.M.S., Mokhtar, Y., Heireche, H., Bousahla, A.A., Tounsi, A. and Mahmoud, S.R. (2018), "A novel shear deformation theory for buckling analysis of single layer graphene sheet based on nonlocal elasticity theory", *Smart Struct. Syst.*, **21**(4) 397-405.

Ahouel, M., Houari, M.S.A., Bedia, E.A.A. and Tounsi, A. (2016), "Size-dependent mechanical behavior of functionally graded trigonometric shear deformable nanobeams including neutral surface position concept", *Steel Compos. Struct.*, **20**(5), 963-981.

Aifantis, E.C. (1992), "On the role of gradients in the localization of deformation and fracture", *Int. J. Eng. Sci.*, **30**(10), 1279-1299.

Al-Basyouni, K.S., Tounsi, A. and Mahmoud, S.R. (2015), "Size dependent bending and vibration analysis of functionally graded micro beams based on modified couple stress theory and neutral surface position", *Compos. Struct.*, **125**, 621-630.

Ansari, R., Hasrati, E. and Gholami, R. (2015), "Nonlinear analysis of forced vibration of nonlocal third-order shear deformable beam model of magneto-electro-thermo elastic nanobeams", *Compos. Part B.*, **83**, 226-241.

Attia, A., Bousahla, A.A., Tounsi, A., Mahmoud, S.R. and Alwabli, A.S. (2018), "A refined four variable plate theory for thermoelastic analysis of FGM plates resting on variable elastic foundations", *Struct. Eng. Mech.*, **65**(4), 453-464.

Bekir, A. and Ömer, C. (2011), "Strain gradient elasticity and modified couple stress models for buckling analysis of axially loaded micro-scaled beams", *Int. J. Eng. Sci.*, **49**(11), 1268-1280.

Bekir, A. and Oumlmer, C. (2013), "Longitudinal vibration analysis of strain gradient bars made of functionally graded materials (FGM)", *Compos. Part B: Eng.*, **55**(55), 263-268.

Bekir, A. and Ömer, C. (2014), "Longitudinal vibration analysis for microbars based on strain gradient elasticity theory", *J. Vibr. Contr.*, **20**(4), 606-616.

Belabed, Z., Bousahla, A.A., Houari, M.S.A., Tounsi, A. and Mahmoud, S.R. (2018), "A new 3-unknown hyperbolic shear deformation theory for vibration of functionally graded sandwich plate", *Earthq. Struct.*, **14**(2), 103-115.

Bellifa, H., Benrahou, K.H., Hadji, L., Houari, M.S.A. and Tounsi, A. (2016), "Bending and free vibration analysis of functionally graded plates using a simple shear deformation theory and the concept the neutral surface position", *J. Braz. Soc. Mech. Sci. Eng.*, **38**(1), 265-275.

Beldjelili, Y., Tounsi, A. and Mahmoud, S.R. (2016), "Hygro-thermo-mechanical bending of s-fgm plates resting on variable elastic foundations using a four-variable trigonometric plate theory", *Smart Struct. Syst.*, **18**(4), 755-786.

Belabed, Z., Houari, M.S.A., Tounsi, A., Mahmoud, S.R. and Bég, O.A. (2014), "An efficient and simple higher order shear and normal deformation theory for functionally graded material (fgm) plates", *Compos. Part B*, **60**(1), 274-283.

Belkorissat, I., Houari, M.S.A., Tounsi, A., Bedia, E.A.A. and Mahmoud, S.R. (2015), "On vibration properties of functionally graded nano-plate using a new nonlocal refined four variable model", *Steel Compos. Struct.*, **18**(4), 1063-1081.

Bellifa, H., Benrahou, K.H., Bousahla, A.A., Tounsi, A. and Mahmoud, S.R. (2017), "A nonlocal zeroth-order shear deformation theory for nonlinear postbuckling of nanobeams", *Struct. Eng. Mech.*, **62**(6), 695-702.

Bennoun, M., Houari, M.S.A. and Tounsi, A. (2016), "A novel five-variable refined plate theory for vibration analysis of functionally graded sandwich plates", *Mech. Compos. Mater. Struct.*, **23**(4), 423-431.

Besseghier, A., Houari, M.S.A., Tounsi, A. and Mahmoud, S.R. (2017), "Free vibration analysis of embedded nanosize fg plates using a new nonlocal trigonometric shear deformation theory", *Smart Struct. Syst.*, **19**(6), 601-614.

Bouafia, K., Kaci, A. and Houari, M.S.A. (2017), "A nonlocal quasi-3D theory for bending and free flexural vibration behaviors of functionally graded nanobeams", *Smart Struct. Syst.*, **19**(2), 115-126.

Boukhari, A., Atmane, H.A., Tounsi, A., Bedia, E.A.A. and Mahmoud, S.R. (2016), "An efficient shear deformation theory for wave propagation of functionally graded material plates", *Struct. Eng. Mech.*, **57**(5), 837-859.

Bouderba, B., Houari, M.S.A., Tounsi, A. and Mahmoud, S.R.

(2016), "Thermal stability of functionally graded sandwich plates using a simple shear deformation theory", *Struct. Eng. Mech.*, **58**(3), 397-422.

Bouderba, B., Houari, M.S.A. and Tounsi, A. (2013), "Thermomechanical bending response of fgm thick plates resting on winkler-pasternak elastic foundations", *Steel Compos. Struct.*, **14**(14), 85-104.

Bourada, M., Kaci, A., Houari, M.S.A. and Tounsi, A. (2015), "A new simple shear and normal deformations theory for functionally graded beams", *Steel Compos. Struct.*, **18**(2), 409-423.

Bounouara, F., Benrahou, K.H., Belkorissat, I. and Tounsi, A. (2016), "A nonlocal zeroth-order shear deformation theory for free vibration of functionally graded nanoscale plates resting on elastic foundation", *Steel Compos. Struct.*, **20**(2), 227-249.

Bousahla, A.A., Mohammed, S.A.H., Abdelouahed, T. and Elabbas, A.B. (2014), "A novel higher order shear and normal deformation theory based on neutral surface position for bending analysis of advanced composite plates", *Int. J. Comput. Meth.*, **11**(6), 1350082.

Bousahla, A.A., Benyoucef, S., Tounsi, A. and Mahmoud, S.R. (2016), "On thermal stability of plates with functionally graded coefficient of thermal expansion", *Struct. Eng. Mech.*, **60**(2), 313-335.

Chaht, F.L., Kaci, A., Houari, M.S.A., Tounsi, A., Beg, O.A. and Mahmoud, S.R. (2015), "Bending and buckling analyses of functionally graded material (fgm) size-dependent nanoscale beams including the thickness stretching effect", *Steel Compos. Struct.*, **18**(2), 425-442.

Dai, H., Yue, X. and Yuan, J. (2014), "A time domain collocation method for studying the aeroelasticity of a two dimensional airfoil with a structural nonlinearity", *J. Comput. Phys.*, **270**(3), 214-237.

Dai, H.L., Rao, Y.N. and Dai, T. (2016), "A review of recent researches on fgm cylindrical structures under coupled physical interactions, 2000-2015", *Compos. Struct.*, **152**, 199-225.

Dohmann, F. and Hartl, C. (1997)," Tube hydroforming-research and practical application", *J. Mater. Proc. Tech.*, **71**(1), 174-186.

Dresselhaus, M.S, Dresselhaus, G., Charlier, J.C. and Hernandez, E. (2004), "Electronic, thermal and mechanical properties of carbon nanotubes", *Philosoph. Trans. Roy. Soc.* A., **362**(1823), 2065-2098.

Ebrahimi, F. and Barati, M.R. (2017), "Longitudinal varying elastic foundation effects on vibration behavior of axially graded nanobeams via nonlocal strain gradient elasticity theory", *Mech. Adv. Mater. Struct.*, **25**(11), 953-963.

Ebrahimi, F. and Javari, A. (2016), "Thermo-mechanical vibration analysis of temperature-dependent porous FG beams based on Timoshenko beam theory", *Struct. Eng. Mech.*, **59**(2), 343-371.

El-Haina, F., Bakora, A., Bousahla, A.A., Tounsi, A. and Mahmoud, S.R. (2017), "A simple analytical approach for thermal buckling of thick functionally graded sandwich plates", *Struct. Eng. Mech.*, **63**(5), 585-595.

Eringen, A.C. (1972), "Nonlocal polar elastic continua", *Int. J. Eng. Sci.*, **10**(1), 1-16.

Eringen, A.C. (1983), "On differential equations of nonlocal elasticity and solutions of screw dislocation and surface waves", *J. App. Phys.*, **54**(9), 4703-4710.

Faghidian, S.A. (2018), "Integro-differential nonlocal theory of elasticity", *Int. J. Eng. Sci.*, **129**, 96-110.

Fernández-Sáez, J., Zaera, R. and Loya, J.A. (2016), "Bending of Euler-Bernoulli beams using Eringen's integral formulation: A paradox resolved", *Int. J. Eng. Sci.*, **99**, 107-116.

Fleck, N.A. and Hutchinson, J.W. (2001), "A phenomenological theory for strain gradient effects in plasticity", *J. Mech. Phys. Sol.*, **41**(12), 1825-1857.

Gan, B.S. (2016), "Post-buckling responses of elastoplastic FGM beams on nonlinear elastic foundation", *Struct. Eng. Mech.*, **58**(3), 515-532.

Ghadiri, M., Rajabpour, A. and Akbarshahi, A. (2017), "Non-linear forced vibration analysis of nanobeams subjected to moving concentrated load resting on a viscoelastic foundation considering thermal and surface effects", *Appl. Math. Model.*, **50**, 676-694.

Ghiasian, S.E., Kiani, Y. and Sadighi, M. (2014), "Thermal buckling of shear deformable temperature dependent circular/annular FGM plates", *Int. J. Mech. Sci.*, **81**(4), 137-148.

Hamidi, A., Houari, M.S.A., Mahmoud, S.R. and Tounsi, A. (2015), "A sinusoidal plate theory with 5-unknowns and stretching effect for thermomechanical bending of functionally graded sandwich plates", *Steel Compos. Struct.*, **18**(1), 235-253.

Hamzacherif, R., Meradjah, M., Zidour, M., Tounsi, A., Belmahi, S. and Bensattalah, T. (2018), "Vibration analysis of nanobeam using differential transform method including thermal effect", *J. Nano Res.*, **54**, 1-14.

Hall, K.C., Thomas, J.P. and Clark, W.S. (2002), "Computation of unsteady nonlinear flows in cascades using a harmonic balance technique", *AIAA. J.*, **40**(5), 879-886.

Hichem, B., Bakora, A., Tounsi, A., Bousahla, A.A. and Mahmoud, S. R. (2017), "An efficient and simple four variable refined plate theory for buckling analysis of functionally graded plates", *Steel Compos. Struct.*, **25**(3), 257-270.

Houari, M.S.A., Tounsi, A., Bessaim, A. and Mahmoud, S.R. (2016), "A new simple three-unknown sinusoidal shear deformation theory for functionally graded plates", *Steel Compos. Struct.*, **22**(2), 257-276.

Hu, W., Song, M. and Deng, Z. (2017), "Axial dynamic buckling analysis of embedded single-walled carbon nanotube by complex structure-preserving method", *Appl. Math. Model.*, **52**, 15-27.

Huang, Y. and Li, X.F. (2010), "Bending and vibration of circular cylindrical beams with arbitrary radial nonhomogeneity", *Int. J. Mech. Sci.*, **52**(4), 595-601.

Jha, D.K., Kant, T. and Singh, R.K. (2013), "A critical review of recent research on functionally graded plates", *Compos. Struct.*, **96**(4), 833-849.

Kaci, A., Houari, M., Bousahla, A.A., Tounsi, A. and Mahmoud, S.R. (2018), "Post-buckling analysis of shear-deformable composite beams using a novel simple two-unknown beam theory", *Struct. Eng. Mech.*, **65**(5), 621-631.

Karami, B., Janghorban, M. and Tounsi, A. (2018a), "Variational approach for wave dispersion in anisotropic doubly-curved nanoshells based on a new nonlocal strain gradient higher order shell theory", *Thin Wall. Struct.*, **129**, 251-264.

Karami, B., Janghorban, M. and Tounsi, A. (2018b), "Nonlocal strain gradient 3d elasticity theory for anisotropic spherical nanoparticles", *Steel Compos. Struct.*, **27**(2), 201-216.

Karami, B., Janghorban, M. and Tounsi, A. (2017), "Effects of triaxial magnetic field on the anisotropic nanoplates", *Steel Compos. Struct.*, **25**(3), 361-374.

Khetir, H., Bouiadjra, M.B., Houari, M.S.A., Tounsi, A. and Mahmoud, S.R. (2017), "A new nonlocal trigonometric shear deformation theory for thermal buckling analysis of embedded nanosize fg plates", *Struct. Eng. Mech.*, **64**(4), 391-402.

Koizumi, M. (1997), "FGM activities in Japan", *Compos. Part B: Eng.*, **28**(1-2), 1-4.

Khodabakhshi, P. and Reddy, J.N. (2015), "A unified integro-differential nonlocal model", *Int. J. Eng. Sci.*, **95**, 60-75.

Lam, D.C.C., Yang, F. and Chong, A.C.M. (2003), "Experiments and theory in strain gradient elasticity", *J. Mech. Phys. Sol.*, **51**(8), 1477-1508.

Li, X., Li, L. and Hu, Y. (2017), "Bending, buckling and vibration of axially functionally graded beams based on nonlocal strain

gradient theory", *Compos. Struct.*, **165**, 250-265.
Li, L., Hu, Y. and Li, X. (2016), "Longitudinal vibration of size-dependent rods via nonlocal strain gradient theory", *Int. J. Mech. Sci.*, **115**, 135-144.
Li, Y.S. and Pan, E. (2015), "Static bending and free vibration of a functionally graded piezoelectric microplate based on the modified couple-stress theory", *Int. J. Eng. Sci.*, **97**, 40-59.
Lim, C.W., Zhang, G. and Reddy, J.N. (2015), "A higher-order nonlocal elasticity and strain gradient theory and its applications in wave propagation", *J. Mech. Phys. Sol.*, **78**, 298-313.
Liu, L., Dowell, E.H. and Hall, K.C. (2007), "A novel harmonic balance analysis for the van der pol oscillator", *Int. J. Nonlin. Mech.*, **42**(1), 2-12.
Liu, L. and Dowell, E.H. (2004), "The secondary bifurcation of an aeroelastic airfoil motion: Effect of high harmonics", *Nonlin. Dyn.*, **37**(1), 31-49.
Lim, C.W., Zhang, G. and Reddy, J.N. (2015), "A higher-order nonlocal elasticity and strain gradient theory and its applications in wave propagation", *J. Mech. Phys. Sol.*, **78**, 298-313.
Lu, L., Guo, X. and Zhao, J. (2017), "Size-dependent vibration analysis of nanobeams based on the nonlocal strain gradient theory", *Int. J. Eng. Sci.*, **116**, 12-24.
Ma, H.M., Gao, X.L. and Reddy, J.N. (2008), "A microstructure-dependent Timoshenko beam model based on a modified couple stress theory", *J. Mech. Phys. Sol.*, **56**(12), 3379-3391.
Mahi, A., Bedia, E.A.A. and Tounsi, A. (2015), "A new hyperbolic shear deformation theory for bending and free vibration analysis of isotropic, functionally graded, sandwich and laminated composite plates", *Appl. Math. Model.*, **39**(9), 2489-2508.
Menasria, A., Bouhadra, A., Tounsi, A., Bousahla, A.A. and Mahmoud, S.R. (2017), "A new and simple HSDT for thermal stability analysis of FG sandwich plates", *Steel Compos. Struct.*, **25**(2), 157-175.
Meziane, M.A.A., Abdelaziz, H.H. and Tounsi, A. (2014), "An efficient and simple refined theory for buckling and free vibration of exponentially graded sandwich plates under various boundary conditions", *J. Sandw. Struct. Mater.*, **16**(3), 293-318.
Merdaci, S., Tounsi, A. and Bakora, A. (2016), "A novel four variable refined plate theory for laminated composite plates", *Steel Compos. Struct.*, **22**(4), 713-732.
Mouffoki, A., Bedia, E.A.A., Houari, M.S.A., Tounsi, A. and Mahmoud, S.R. (2017), "Vibration analysis of nonlocal advanced nanobeams in hygro-thermal environment using a new two-unknown trigonometric shear deformation beam theory", *Smart Struct. Syst.*, **20**(3), 369-383.
Mouffoki, A., Bedia, E.A.A., Houari, M.S.A., Tounsi, A. and Mahmoud, S.R. (2017), "Vibration analysis of nonlocal advanced nanobeams in hygro-thermal environment using a new two-unknown trigonometric shear deformation beam theory", *Smart Struct. Syst.*, **20**(3), 369-383.
Mook, D. and Nayfeh, A. (1979), *Nonlinear Oscillations*, John Wiley & Sons, New York, U.S.A.
Mindlin, R.D. (1964), "Micro-structure in linear elasticity", *Arch. Ration. Mech. Anal.*, **16**(1), 51-78.
Mindlin, R.D. (1965), "Second gradient of strain and surface-tension in linear elasticity", *Int. J. Sol. Struct.*, **1**(4), 417-438.
Nazemnezhad, R. and Hosseini-Hashemi, S. (2014), "Nonlocal nonlinear free vibration of functionally graded nanobeams", *Compos. Struct.*, **110**(110), 192-199.
Rahmani, O. and Pedram, O. (2014), "Analysis and modeling the size effect on vibration of functionally graded nanobeams based on nonlocal Timoshenko beam theory", *Int. J. Eng. Sci.*, **77**(7), 55-70.
Rahaeifard, M. (2015), "Size-dependent torsion of functionally graded bars", *Compos. Part B*, **82**, 205-211.
Reddy, J.N., Romanoff, J. and Loya, J.A. (2015), "Nonlinear finite element analysis of functionally graded circular plates with modified couple stress theory", *Eur. J. Mech. A/Sol.*, **56**, 92-104.
Reddy, J.N. and Chin, C.D. (1998), "Thermomechanical analysis of functionally graded cylinders and plates", *J. Therm. Stress.*, **21**(6), 593-626.
Salehipour, H., Shahidi, A.R. and Nahvi, H. (2015), "Modified nonlocal elasticity theory for functionally graded materials", *Int. J. Eng. Sci.*, **90**, 44-57.
Sahmani, S., Aghdam, M.M. and Rabczuk, T. (2018), "Nonlocal strain gradient plate model for nonlinear large-amplitude vibrations of functionally graded porous micro/nano-plates reinforced with GPLs", *Compos. Struct.*, **198**, 51-62.
She, G.L., Ren, Y.R. and Yuan, F.G. (2018), "On vibrations of porous nanotubes", *Int. J. Eng. Sci.*, **125**, 23-35.
She, G.L., Yuan, F.G. and Ren, Y.R. (2017), "On buckling and postbuckling behavior of nanotubes", *Int. J. Eng. Sci.*, **121**, 130-142.
She, G.L, Yuan, F.G. and Ren, Y.R. (2018), "On wave propagation of porous nanotubes", *Int. J. Eng. Sci.*, **130**, 62-74.
Shen, H.S. and Wang, Z.X. (2014), "Nonlinear analysis of shear deformable FGM beams resting on elastic foundations in thermal environments", *Int. J. Mech. Sci.*, **81**(4), 195-206.
Şimşek, M., Aydın, M. and Yurtcu, H. (2015), "Size-dependent vibration of a microplate under the action of a moving load based on the modified couple stress theory", *Acta. Mech.*, **226**(11), 3807-3822.
Tounsi, A., Houari, M.S.A. and Benyoucef, S. (2013), "A refined trigonometric shear deformation theory for thermoelastic bending of functionally graded sandwich plates", *Aerosp. Sci. Technol.*, **24**(1), 209-220.
Tuna, M. and Kirca, M. (2016), "Exact solution of Eringen's nonlocal integral model for bending of Euler-Bernoulli and Timoshenko beams", *Int. J. Eng. Sci.*, **105**, 80-92.
Tsiatas, G.C. (2009), "A new Kirchhoff plate model based on a modified couple stress theory", *Int. J. Sol. Struct.*, **46**(13), 2757-2764.
Yang, F., Chong, A.C.M. and Lam, D.C.C. (2002), "Couple stress based strain gradient theory for elasticity", *Int. J. Sol. Struct.*, **39**(10), 2731-2743.
Yang, F., Chong, A.C.M. and Lam, D.C.C. (2009), "Couple stress based strain gradient theory for elasticity", *Int. J. Sol. Struct.*, **39**(10), 2731-2743.
Yazid, M., Heireche, H., Tounsi, A., Bousahla, A.A. and Houari, M.S.A. (2018), "A novel nonlocal refined plate theory for stability response of orthotropic single-layer graphene sheet resting on elastic medium", *Smart Struct. Syst.*, **21**(1), 15-25.
Yahia, S.A., Atmane, H.A., Houari, M.S.A. and Tounsi, A. (2015), "Wave propagation in functionally graded plates with porosities using various higher-order shear deformation plate theories", *Struct. Eng. Mech.*, **53**(6), 1143-1165.
Youcef, D.O., Kaci, A., Benzair, A., Bousahla, A.A. and Tounsi, A. (2018), "Dynamic analysis of nanoscale beams including surface stress effects", *Smart Struct. Syst.*, **21**(1), 65-74.
Younsi, A., Tounsi, A., Zaoui, F.Z., Bousahla, A.A. and Mahmoud, S.R. (2018), "Novel quasi-3D and 2D shear deformation theories for bending and free vibration analysis of FGM plates", *Geomech. Eng.*, **14**(6), 519-532.
Zaoui, F.Z., Ouinas, D. and Tounsi, A. (2019), "New 2D and quasi-3D shear deformation theories for free vibration of functionally graded plates on elastic foundations", *Compos. Part B*, **159**, 231-247.
Zemri, A., Houari, M.S.A., Bousahla, A.A. and Tounsi, A. (2015), "A mechanical response of functionally graded nanoscale beam: An assessment of a refined nonlocal shear deformation theory beam theory", *Struct. Eng. Mech.*, **54**(4), 693-710.
Zhang, P. and Fu, Y. (2013), "A higher-order beam model for

tubes", *Eur. J. Mech. A/Sol.*, **38**, 12-19.
Zhang, X.M., Liu, G.R. and Lam, K.Y. (2001), "Vibration analysis of thin cylindrical shells using wave propagation approach", *J. Sound Vibr.*, **239**(3), 397-403.
Zhong, J., Fu, Y. and Wan, D. (2016), "Nonlinear bending and vibration of functionally graded tubes resting on elastic foundations in thermal environment based on a refined beam model", *Appl. Math. Mod.*, **40**(17-18), 7601-7614.
Zidi, M., Tounsi, A., Houari, M.S.A., Bedia, E.A.A. and Bég, O.A. (2014), "Bending analysis of fgm plates under hygro-thermo-mechanical loading using a four variable refined plate theory", *Aerosp. Sci. Technol.*, **34**(4), 24-34.
Zidi, M., Houari, M.S.A., Tounsi, A., Bessaim, A. and Mahmoud, S.R. (2017), "A novel simple two-unknown hyperbolic shear deformation theory for functionally graded beams", *Struct. Eng. Mech.*, **64**(2), 145-153
Zouatnia, N., Hadji, L. and Kassoul, A. (2017), "A refined hyperbolic shear deformation theory for bending of functionally graded beams based on neutral surface position", *Struct. Eng. Mech.*, **63**(5), 683-689.

PL